

INVESTIGATION OF THE INTERACTION BETWEEN ANTIMICROBIAL
PEPTIDES AND LIPID MEMBRANES USING ION MOBILITY MASS
SPECTROMETRY COUPLED WITH ISOTHERMAL TITRATION CALORIMETRY

A Thesis

by

ANQI CHEN

Submitted to the Office of Graduate and Professional Studies of
Texas A&M University
in partial fulfillment of the requirements for the degree of

MASTER OF SCIENCE

Chair of Committee,	David H. Russell
Committee Members,	Christian B. Hilty
	J. Martin Scholtz
Head of Department,	Simon W. North

August 2016

Major Subject: Chemistry

Copyright 2016 Anqi Chen

ABSTRACT

Antimicrobial peptides (AMP) are involved in many biological processes owing to their ability to interact with the cell membranes. The aim of many biophysical methods is to understand the mechanism of AMP function such that their bioactivities can be tailored for therapeutic purposes. There is no single experimental technique that can provide a complete understanding of the mechanism of AMP-bilayer interactions; however, this emphasizes the necessity for a combination of techniques in order to provide a more complete view of cellular processes. In this study, ion mobility mass spectrometry (IM-MS) is coupled with isothermal titration calorimetry (ITC) to study the interaction between antimicrobial peptide gramicidin A (GA) with lipid bilayer as well as between antimicrobial peptide gramicidin S (GS) with lipid bilayer. IM-MS can probe the membrane bound structure of GA and the conformer preferences of GA can be influenced by the physical properties of lipid comprising the bilayer. The information obtained from IM-MS is limited to investigation into structural changes of the peptide and the effects of the peptide on surrounding lipids remain to be resolved. Here, ITC is used as a complementary technique to elucidate the lipid-peptide interactions. ITC is capable of providing a thermodynamic description of the entire binding process of GS to various lipid bilayer model membranes. The thermodynamics of the binding of GS can be affected by the properties of the bilayer, thus it is possible to incorporate small molecules that affect the bilayer physiochemical properties, such as cholesterol, or peptide like GA into the bilayer and study how the presence of these molecules affects

the thermodynamics of GS binding. Also, since the conformer preferences of GA in membrane is sensitive to the lipid structure and composition, and the conformational changes of GA can be probed by IM-MS, it is also possible to use GA as a “reporter” to investigate how binding of GS changes the lipid environment. The mechanism of GA and GS interaction with lipid bilayer can thus be elucidated through combining the information obtained from ITC with that from IM-MS.

DEDICATION

This work is dedicated to my loving grandparents:

Yuhua Zhang

Tailu Chen

Huaying Chen

and

Jie Zhou

ACKNOWLEDGEMENTS

I would like to express my deepest appreciation to my advisor, Dr. David H. Russell, for his constant guidance and support throughout the course of my research. I am so impressed by his wisdom and enthusiasm for science. I will always be grateful.

I would like to thank each of the members in the Russell Research Group for their support and suggestions. Special thanks to John Patrick for teaching me the skills I needed to accomplish my research project; to Yuanyou Wang for her support and guidance on theory and application of isothermal titration calorimetry; to Dr. Kerry Wooding and Nichole Wagner for helpful discussions and guidance on using ion mobility mass spectrometry.

I would also like to thank each of the professors in Chemistry Department under whom I have received lectures and training. I also want to thank Dr. Christian Hilty and Dr. Martin Scholtz for agreeing to serve on my defense committee.

Thanks also go to all my friends for making my time at Texas A&M University a great experience. Finally, thanks to my mother and father for their endless love and to my boyfriend Zhengyang Jiang, who is always with me during my struggles. I would never have been able to survive graduate school without their encouragement.

NOMENCLATURE

AMP	antimicrobial peptide
GA	Gramicidin A
GS	Gramicidin S
IM-MS	Ion Mobility Mass Spectrometry
VCFD	vesicle capture-freeze-drying
CCS	Collision Cross Section
ITC	Isothermal Titration Calorimetry
ESI	Electrospray Ionization
POPC	1-palmitoyl-2-oleoyl- <i>sn</i> -glycero-3-phosphocholine
POPG	1-hexadecanoyl-2-(9Z-octadecenoyl)- <i>sn</i> -glycero-3-phospho-(1'-rac-glycerol)
DLPC	1,2-dilauroyl- <i>sn</i> -glycero-3-phosphocholine
DMPC	1,2-dimyristoyl- <i>sn</i> -glycero-3-phosphocholine
DEPC	dielaidoylphosphatidylcholine
SSHH	single stranded head-to-head dimer
PDH	parallel double helix
ADH	antiparallel double helix
N	binding stoichiometry
K_a	binding constant
K_d	dissociation constant

ΔH	binding enthalpy
ΔS	binding entropy
B_{\max}	maximal binding capacity

TABLE OF CONTENTS

	Page
ABSTRACT	ii
DEDICATION	iv
ACKNOWLEDGEMENTS	v
NOMENCLATURE	vi
TABLE OF CONTENTS	viii
LIST OF FIGURES	x
LIST OF TABLES	xii
CHAPTER I INTRODUCTION	1
CHAPTER II METHODS	6
Lipid vesicle preparation	6
Vesicle Capture-Freeze-Drying (VCFD)	7
Isothermal Titration Calorimetry (ITC)	8
Ion Mobility Mass Spectrometry (IM-MS)	12
CHAPTER III EFFECTS OF CHOLESTEROL ON THE BINDING OF GRAMICIDIN S TO LIPID BILAYERS STUDIED BY ISOTHERMAL TITRATION CALORIMETRY	15
Introduction	15
Experimental methods	17
Results and discussion	17
Conclusions	28
CHAPTER IV EFFECTS OF GRAMICIDIN A ON THE BINDING OF GRAMICIDIN S TO LIPID BILAYERS STUDIED BY ISOTHERMAL TITRATION CALORIMETRY	30
Introduction	30
Experimental methods	34

Results and discussion	35
Conclusions	42
CHAPTER V ION MOBILITY MASS SPECTROMETRY STUDIES OF CONFORMATIONAL CHANGES OF GRAMICIDIN A INDUCED BY THE BINDING OF GRAMICIDIN S	44
Introduction	44
Experimental methods	45
Results and discussions	46
Conclusions	50
CHAPTER VI SUMMARY	52
REFERENCES	54

LIST OF FIGURES

	Page
Figure 1 Vesicle Capture-Freeze-Drying (VCFD).....	7
Figure 2 Results of a characteristic titration experiment (upper panel) with the associated data analysis (lower panel).....	9
Figure 3 Schematic representation of an isothermal titration calorimeter	10
Figure 4 The shape of the binding isotherm as a function of the c-value	11
Figure 5 A schematic diagram of the ion-mobility drift tube.....	13
Figure 6 Different stages of peptide binding.....	16
Figure 7 ITC experimental data at 25 °C. 20 × 2 μL of 19.7 mM POPC/Cholesterol (10:4) was injected into 280 μL sample cell containing 50 μM GS. Data analysis was performed using Origin with built-in curve fitting models	18
Figure 8 Binding isotherm for the binding of GS to lipid vesicles containing 40% of cholesterol derived from the ITC measurement at 25 °C. Data analysis was performed using Origin with built-in curve fitting models.	22
Figure 9 ITC experimental data of POPC LUV containing various amounts of cholesterol injected into GS. (Red: 40%, Green: 20% and Blue: 0%). Data analysis was performed using Origin with built-in curve fitting models.	24
Figure 10 Binding isotherms for the binding of GS to lipid vesicles containing various amounts of cholesterol derived from the ITC measurement at 25 °C (Red: 40%, Green: 20% and Blue: 0%). Data analysis was performed using Origin without built-in curve fitting models.	25
Figure 11 Lipid bilayer without and with cholesterol (Blue: hydration layer)	27
Figure 12 Different conformations of Gramicidin A (A: N-terminal to N-terminal head-to-head dimer; B: C-terminal to C-terminal head-to-head dimer; C: antiparallel double helice; and D: parallel double helice).....	30
Figure 13 CCS profiles of GA [2 M + 2 Na] ²⁺ incorporated in 100 nm lipid vesicles formed using (A) DLPC (12:0 PC) (B) DMPC (14:0 PC) (C) POPC (16:0, 18:1 PC) (D) DEPC (22:1 PC)	32

Figure 14	Collision cross section (CCS) profiles of GA (upper panel) and deformedylated GA (lower panel) in POPC lipid vesicle.....	36
Figure 15	(A) ITC experimental data of POPC LUV with (red) and without (black) GA bound injected into GS solution. (B) ITC experimental data of POPC LUV with GA (red) / deformedylated GA (blue) bound injected into GS. Molar ratio between POPC and GA (deformedylated GA) was 100:1.....	37
Figure 16	Binding isotherms for the binding of GS to lipid vesicles with GA (red) and dGA (blue) bound as well as no GA/deformedylated GA bound (control: black). Data analysis was performed using Origin 8.5.1.....	38
Figure 17	Effects of N-terminus deformedylation on GA-lipid interactions ((A) Before deformedylation; (B) After deformedylation; Blue: hydration layer)	41
Figure 18	CCS profiles of GA dimer $[2 M + 2Na^+]$ in POPC lipid vesicles with various amounts of GS bound	47
Figure 19	Plots of relative abundances of the three GA dimers as a function of GS/lipid molar ratios	49

LIST OF TABLES

	Page
Table 1 Thermodynamic parameters for the binding of GS to lipid vesicles containing 40% of cholesterol.....	22
Table 2 Thermodynamic parameters for the binding between GS and POPC LUV containing various amounts of cholesterol obtained using Origin with (upper panel) and without (lower panel) built-in curve fitting models respectively. ...	26
Table 3 Thermodynamic parameters for the binding between GS and POPC LUV with and without GA (deformylated GA)	39

CHAPTER I

INTRODUCTION

Membrane-active peptides are attracting a growing interest since they are involved in many crucial biological processes. Antimicrobial peptides (AMPs) are a large family of membrane active peptides that exhibit a broad range of bioactivities, *i.e.*, disturb bilayer integrity either by disruption of pore formation.¹ They are an important class of peptides owing to their ability to lyse bacterial cell walls. For many natural AMPs, they act by disrupting the integrity of cell membranes through strong interactions with phospholipid bilayers. Currently, AMPs (e.g., Cecropins,² Melittin,³ and Gramicidins⁴) have been used as drug candidates against many diseases since they exhibit a variety of antibiotic activities. As the widespread increase in antibiotic resistance of bacteria and fungi becomes a growing human-health related problem, it is of paramount important to understand the structure-function relationship of these peptides, which allow us to design peptide analogues with tailored functionalities.^{1,5}

To understand the functional mechanism of the interaction between AMPs and membranes, several issues need to be addressed such as secondary structure, orientation, oligomerization and localization of AMPs associated with the lipid bilayer. At the same time, the effects of the insertion/binding of AMPs to membranes on the physico-chemical properties of lipid bilayers also need to be elucidated.¹ Several biophysical techniques have been developed to study the membrane-peptide systems, *i.e.*, fluorescence,⁶ electron paramagnetic resonance spectroscopy (EPR),⁷ infrared

spectroscopy (IR),⁸ circular dichroism (CD),⁹ surface plasmon resonance (SPR),¹⁰ X-ray,¹¹ and NMR^{12,13} have been used to characterize the dynamics and structure of peptides and lipids upon binding. Computational methods have also been widely used for studying peptide-membrane interactions.^{14,15} The combination of different biophysical studies of membrane interacting peptides can provide complementary information, however, each technique has its own limitation: EPR requires the sample to be chemically modified which is laborious and may influence its behavior in the hydrophobic environment;¹⁶ For X-ray diffraction, it is hard to get detailed insights into peptide-membrane systems because of the lack of long-range crystalline order;¹¹ NMR usually takes a long data acquisition time and high quantities of sample, and the spectral complexity makes the data analysis difficult and time consuming.^{12,13} As a result, the structural characterization of membrane active peptides in the lipid bilayer is always a harsh experimental challenge.

Gramicidin A (GA) is a linear antimicrobial peptide that can form ion-conducting channels across membranes.¹⁷ The amino acid sequence of GA is: HCO-L-Val-Gly-L-Ala-D-Leu-L-Ala-D-Val-L-Val-D-Val-L-Trp-D-Leu-L-Trp-D-Leu-L-Trp-D-Leu-L-Trp-NHCH₂CH₂OH.¹⁸ The lack of basic residues in the sequence makes GA extremely hydrophobic and almost insoluble in water. Additionally, alternating L- and D- amino acids results in the side chains protruding from the same side of the molecules, contributing to its low solubility in water.¹⁹ It has been proposed from early NMR studies that a channel is formed by head-to-head dimerization of two GA monomers, each in a single stranded helical conformation.²⁰ More recent NMR studies revealed that

head-to-head dimers may not be the only conformations of GA in membranes, small amounts of double helices or other conformations may coexist with the head-to-head dimer.²¹ Owing to the similar physical characteristics of the different conformations of GA dimer, distinguishing between these structures is difficult.²² As a result, the extent of structural heterogeneity of GA dimers in lipid bilayers remains unresolved.

Patrick *et al.* have demonstrated that ion-mobility mass spectrometry (IM-MS) is a novel method that can probe the membrane-bound structure of GA.²³ Here, a novel sample preparation method, vesicle capture-freeze-drying (VCFD) is coupled with IM-MS to preserve the membrane-bound structure of GA. The lipid vesicles are prepared in the presence of GA such that hydrophobic GA molecules are entrapped in the lipid bilayers. The vesicle samples with GA bounded are then resuspended in isobutanol prior to be analyzed by IM-MS. Using this method, different conformations of GA dimers can be resolved from the collision cross section (CCS) profiles. It has been shown that there is a significant abundance of antiparallel double helices (ADH) and parallel double helices (PDH) that coexist with the single-stranded head-to-head dimer (SSHH) and the conformer preferences of GA dimers are sensitive to the physical properties of the lipid composing the bilayer, *i.e.*, acyl chain length and degree of unsaturation.²³ This suggests that to some extent, the membrane-bound conformations of GA dimers can be preserved when transferred from solution-phase into the gas-phase.

IM-MS alone does not provide information for the complete structural picture of the interaction between GA and the lipid vesicles. Only the conformational distribution of GA dimers can be probed by IM-MS, other information such as the location of GA

associated with the membrane, whether it is inserted into the membrane or floating on the surface of the membrane remains unclear. It is necessary to combine IM-MS with other techniques to fully elucidate GA-lipid interactions. Here, isothermal titration calorimetry (ITC) is selected as a complementary technique to IM-MS in characterizing the interaction between antimicrobial peptides and lipid vesicles. There are several advantages when using ITC: (i) the high sensitivity of ITC allows measurements of the binding of peptide solutions to lipid bilayers in micromolar concentration range; (ii) nearly all the chemical processes are accompanied by the absorption or release of heat, removing any necessity for chemical labeling; (iii) ITC can provide binding isotherms, which can be fit with a specific binding model to generate thermodynamic parameters.²⁴

Gramicidin S (GS) is a cationic cyclic antimicrobial peptide that exhibits high lytic activity against a broad spectrum of both Gram-positive and Gram-negative bacteria. The GS molecule is amphiphilic, having two polar and charged Orn side chain and two D-Phe in the ring as well as four hydrophobic Val and Leu side chains. Previous studies revealed that GS lyses bacteria by permeabilizing and destabilizing their inner membranes.²⁵ A number of biophysical studies have been carried out to determine the molecular mechanism of the action of GS. Abraham *et al.* have shown that ITC is capable of providing a thermodynamic description of the whole binding process of GS to various lipid bilayer model membrane systems.²⁶ The binding isotherm could be described by a one-site binding model. They used ITC to study the binding between GS and lipid vesicles composed of the zwitterionic lipid POPC or the anionic lipid POPG, with and without cholesterol. The results revealed that the binding is primarily entropy-

driven with a positive ΔS value. POPG can bind to GS with both a higher binding affinity and a higher binding capacity than POPC. This is not surprising, as the electrostatic interactions between positively charged residue (Orn) and negatively charged glycerol headgroups on POPG should facilitate peptide binding. The presence of cholesterol reduced the binding, which can be explained by a hindered penetration into the cholesterol-containing membrane due to restricted flexibility of the tightly packed hydrocarbon chains.²⁷

Since the binding process of GS can be affected by the composition of the membranes, it is possible to incorporate GA into the bilayer to study how the presence of GA affects the binding of GS, thus providing information on how GA affects the physicochemical properties of the lipid. On the other hand, since the conformation of GA is dependent on the lipid environment, we propose that we could also use GA as a “reporter” to investigate how the binding of GS affects the lipid environment. The changes in the conformer preferences of GA in the lipid vesicles induced by the binding of GS should provide information on how GS binding affects the structure and properties of the lipid bilayers. In this study, IM-MS coupled with ITC is utilized to characterize the interactions between GA and lipid bilayer model system as well as between GS and lipid bilayer model system.

CHAPTER II

METHODS*

Lipid vesicle preparation

POPC lipids were acquired from Avanti Polar Lipids, Alabaster, Alabama, USA. For lipid vesicles containing cholesterol, POPC and cholesterol were co-dissolved in chloroform, whereas for lipid vesicles with no cholesterol, lipids were solely dissolved in chloroform. In both cases, lipid concentrations were 20 mg/ml. Aliquots containing 10-20 mg lipid were portioned out into small vials, dried under N₂ gas to remove chloroform and form thin lipid films. The lipid films were rehydrated with 1.0 ml of 18.0 MΩ water to yield lipid concentrations of 10-20 mg/ml (13.2-26.3 mM). Samples were sonicated 30 minutes at room temperature (above -4 °C, lipid transition temperature for POPC) to yield large multilamellar vesicles (MLV), wherein lipid bilayer were layered around each other and separated by layers of water.²⁸ The lipid suspensions were then freeze-thawed 8 times and forced through a polycarbonate filter with a pore size of 100 nm to yield large unilamellar vesicles (LUV) with a diameter near the pore size. The extrusion was also performed at room temperature. Abraham *et al.* used POPC LUVs with a diameter of 200 nm in the ITC studies.^{25,26} Here, LUVs with a diameter of 100 nm were prepared in order to increase the liposome stability, which decreases with

* Part of this chapter is reprinted with permission from “Elucidation of conformer preferences for a hydrophobic antimicrobial peptide by vesicle capture-freeze-drying: a preparatory method coupled to ion mobility-mass spectrometry” by Patrick, J. W.; Gamez, R. C.; Russell, D. H, **2015**. *Anal Chem*, 87, 578-583, Copyright 2014 by American Chemical Society.

increasing lipid vesicle size.²⁹ Also, cholesterol was included in the lipid vesicles in order to modify the physicochemical properties of the lipid bilayer and investigate its effect on the binding process.

Vesicle Capture-Freeze-Drying (VCFD)

GA peptide was purchased from Sigma-Aldrich St. Louis, Mo, USA and dissolved in ethanol with a concentration of 4.8 mg/ml. Samples of POPC lipid with a concentration of 10-20 mg/ml in chloroform and gramicidin A in ethanol were combined at a molar ratio of 100:1, dried under N₂ gas until solvent was removed. Lipid vesicles were then prepared as previously described in *lipid vesicle preparation*. Since the lipid vesicles were prepared in the presence of GA, the GA molecules were entrapped into the lipid bilayers owing to the extremely hydrophobic character of the GA peptide. After the lipid vesicles loaded with GA were formed, the solutions were allowed to incubate at 4 °C overnight. The vesicle/GA samples were then freeze-dried using liquid nitrogen and a vacuum desiccator to remove water. After that, the samples were rehydrated with isobutanol for ESI-IM-MS analysis (Figure 1).²³

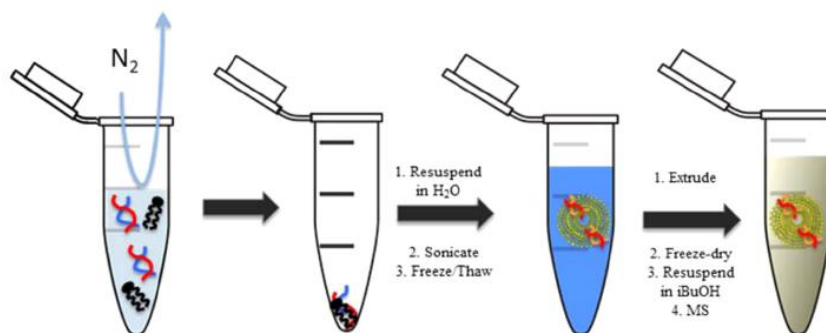


Figure 1. Vesicle Capture-Freeze-Drying (VCFD)

Isothermal Titration Calorimetry (ITC)

ITC is a biophysical technique that can provide a thermodynamic description for a binding process. ITC can provide binding isotherms, which can be fit with a specific binding model to generate thermodynamic parameters. The raw data obtained through multiple injections, as shown in the upper panel of Figure 2 (each spike in heat given off denotes an injection), can be integrated to generate the binding isotherm shown in the lower panel of Figure 2, from which the binding affinity K_a (determined by the slope of the binding isotherm), binding stoichiometry N (reflection point) and the observed binding enthalpy ΔH (maximum amplitude) can be extracted.²⁴

ITC consists of a micro-syringe for sample injections, as well as a sample cell and a reference cell (Figure 3). The binding between a protein and a ligand is measured by loading the sample cell with protein solution and the micro-syringe with ligand solution. During the titration, a small amount of the ligand solution is injected into the sample cell through the micro-syringe. The heat absorbed or released upon binding of the protein with ligand is measured using an electronic feedback system which keeps the reference and sample cells at the same temperature. No heat change occurs in the reference cell as it contains only water. If there is an exothermic binding reaction in the sample cell, a reduction in heating power occurs to minimize the temperature difference between the sample and reference cells. Conversely, an endothermic reaction requires an increase in heating power. The instrument is highly sensitive and can measure heats of reaction of $\sim 1 \mu\text{cal}$.³⁰

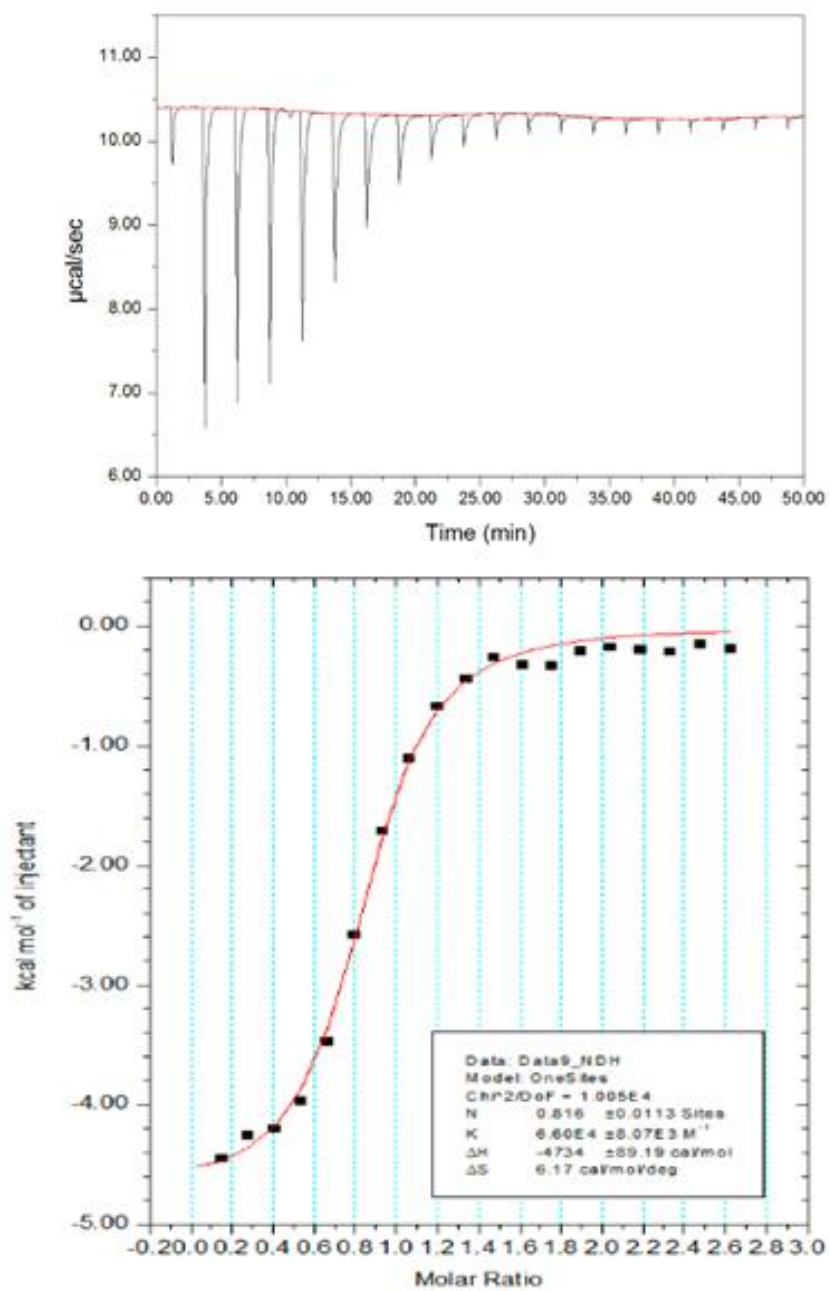


Figure 2. Results of a characteristic titration experiment (upper panel) with the associated data analysis (lower panel).

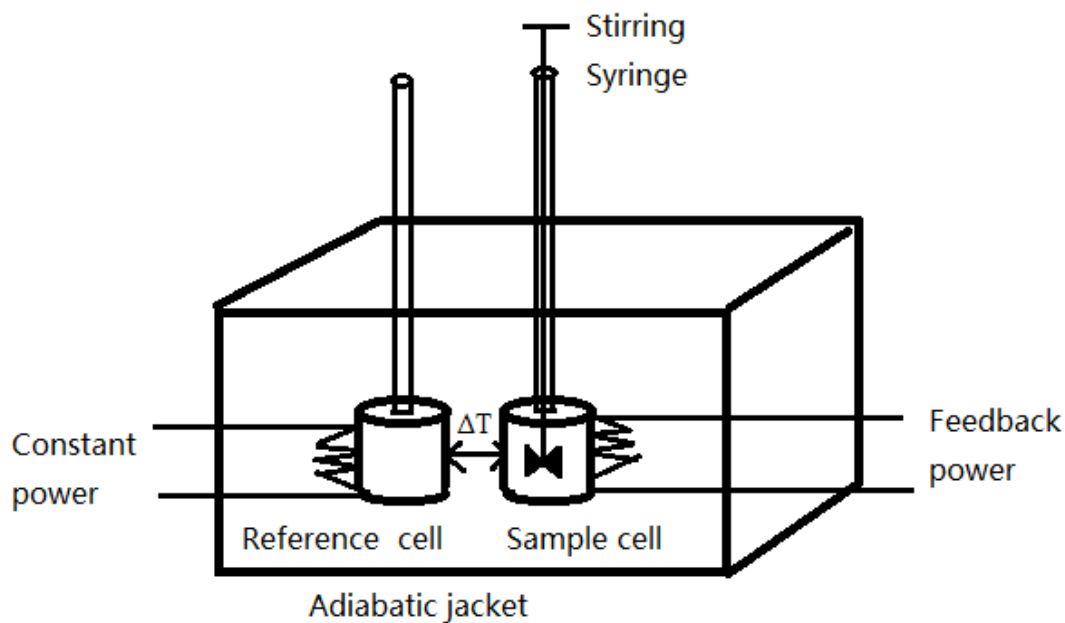


Figure 3. Schematic representation of an isothermal titration calorimeter

The shape of the binding isotherm is determined by several critical parameters which includes initial protein concentration in the sample cell, M_p , the binding constant, K_a , and the binding stoichiometry parameter, N . Wiseman *et al.* has derived the following equation to help in the design of ITC experiment: $c = N \cdot M_p \cdot K_a$. Higher c values result in titration curves that are too steep to resolve K_a accurately, whereas lower c values results in shallow titration curves from which all three parameters N , K_a and ΔH are poorly resolved (Figure 4). To determine the three parameters accurately, it is recommended to perform the ITC experiment where $20 < c < 100$.³¹ For high affinity interactions (high K_a), ITC should be performed at low concentrations; whereas for low

affinity interactions (low K_a), ITC should be performed at high concentrations. If the binding affinity is unknown, several different concentrations of peptide solution should be prepared in order to determine the best experimental condition where the three parameters can be well resolved. At the same time, the ligand concentration in the syringe should be increased with increasing protein concentration in the sample cell in order to keep the same protein/ligand molar ratio where saturation occurs within the first third to half of the titration.

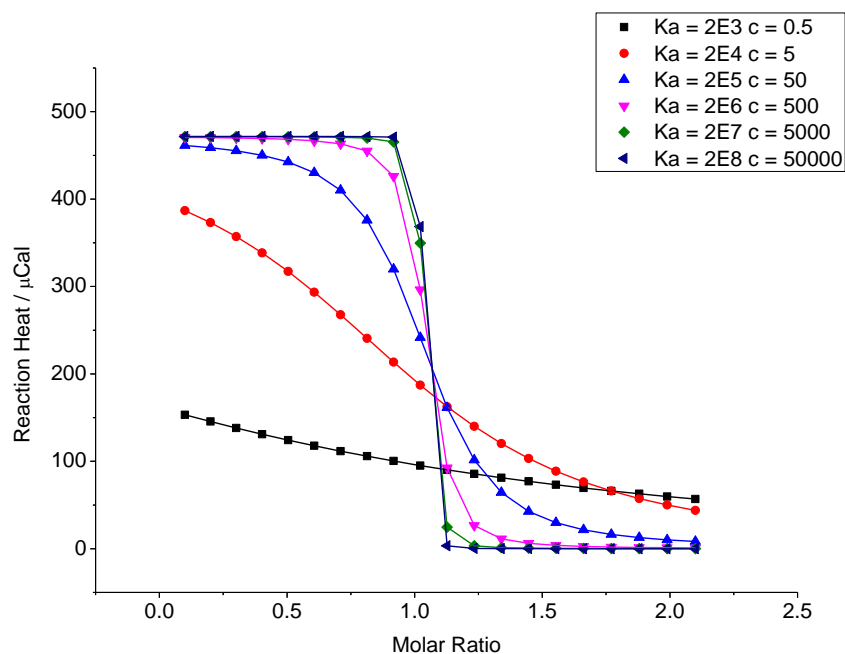


Figure 4. The shape of the binding isotherm as a function of the c -value

Ion Mobility Mass Spectrometry (IM-MS)

Ion mobility is a technique that can separate gas phase ion based on their size and shape. When IM-MS analysis is being performed, the protein or peptide of interested is first ionized by nano-electrospray ionization. After ionization, protein or peptide ions are injected into a drift cell which contains neutral gas at a controlled pressure. The neutral gas is typically nitrogen or helium. Ions will then undergo IM separation under the influence of a relatively weak electric field. For ions with larger shape and size, they will experience more collisions with the neutral gas and thus need more time to travel through the drift cell than smaller ions. Therefore, ions with different size and shape will be separated according to their ion-neutral collision cross-section (Ω). Also, ions with higher charge state will experience stronger electric field strengths and will migrate through the drift cell more quickly than ions with lower charge state. The following equation can be used to convert drift times (t_D) into collision cross-section (Ω output in m^2):

$$\Omega = \frac{(18\pi)^{1/2}}{16} \frac{ze}{(k_b T)^{1/2}} \left[\frac{1}{m_I} + \frac{1}{m_N} \right]^{1/2} \frac{t_D E}{L} \frac{760}{P} \frac{T}{273.2} \frac{1}{N} \quad (1)$$

where k_b is the Boltzmann constant, z is the ion charge, e (C) is the elementary charge, m_I is the mass of the ion, m_N is the mass of the neutral gas (both in kg), E is the electric field strength (V/m), L is the length of the drift region (m), P is pressure (torr), T is temperature (Kelvin), t_D is drift time (seconds, corrected for time spent outside the drift cell) and N is the neutral gas number density (m^{-3}).³²

The coupling of ion mobility with mass spectrometry is referred to as ion mobility-mass spectrometry. Thousands of mass spectra can be obtained for each ion

mobility spectrum producing a two-dimensional array in which both mobility and mass of ions are recorded. One unique feature of IM-MS spectra is that they often exhibit a mass-mobility correlation for classes of ions. These mass-mobility correlations are commonly called ‘trend lines’. This feature allows it to separate different species such as lipids, peptides, carbohydrates and nucleotides in biological samples based on differences in their gas-phase packing efficiencies.³³

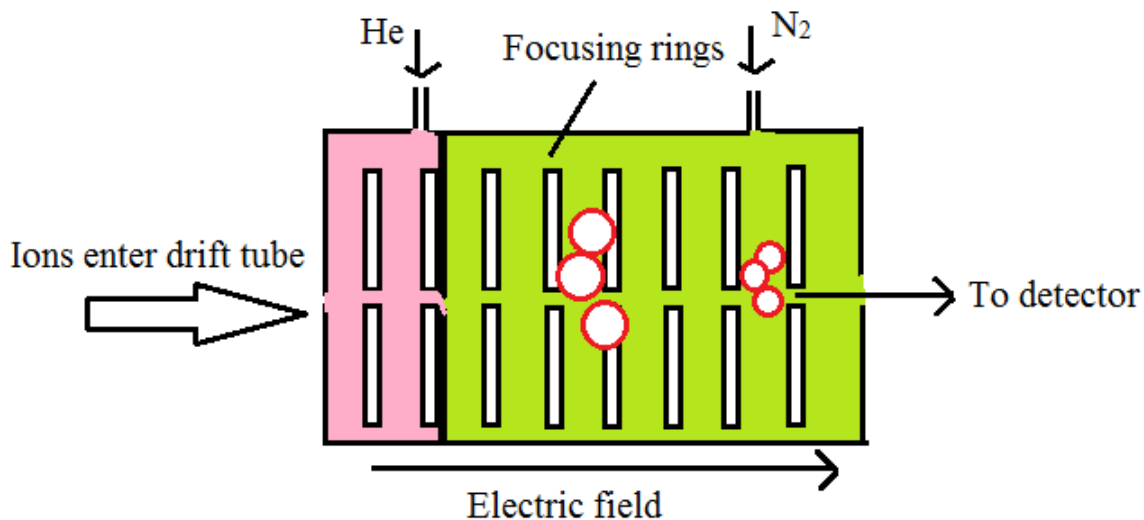


Figure 5. A schematic diagram of the ion-mobility drift tube

In this study, the IM-MS were acquired on a Water Synapt™ HDMS G2 mass spectrometer (Waters Corp., Milford, MA). A schematic diagram of the instrument is shown on Figure 5. Ions were formed by nano-ESI with a source temperature of ~100 °C. The capillary voltage applied to the ESI tips was 1.5-2 kV. The instrument was equipped with a traveling-wave ion mobility cell with 30 V wave height and 300 m/s wave

velocity. Sampling one voltage and extraction cone voltage were set at 15 V and 4 V respectively. The data analysis for IM experiment was performed using MassLynx v4.1 software. The CCS values for GA dimers were obtained using calibration method described previously by Ruotolo *et al.*³² The doubly charged tryptic digest ions of cytochrome C and myoglobin were used as calibrants, and their CCS were obtained from collision cross section database generated by Clemmer and coworkers.³⁴

CHAPTER III

EFFECTS OF CHOLESTEROL ON THE BINDING OF GRAMICIDIN S TO LIPID BILAYERS STUDIED BY ISOTHERMAL TITRATION CALORIMETRY

Introduction

Over the last decade, ITC has become increasingly popular to study lipid-peptide interactions.³⁵ The binding between peptide and bilayer can be divided into two individual steps (Figure 6): First, the positively charged antimicrobial peptide is adsorbed to the negatively charged membrane surface owing to electrostatic attractions; Second, the peptide may remain electrostatically adsorbed at the polar headgroup region of the membrane, or it may insert into the hydrophobic core of the membrane.³⁵ The insertion process could be either enthalpy-driven by van-der-Waals interactions, or could be entropy-driven by hydrophobic effect. Insertion into the lipid membrane is typically accompanied by a conformational change of the peptide.

Gramicidin S (GS) is a cyclic decaameric cationic antimicrobial peptide first isolated from the Gram-positive bacteria *Bacillus brevis*. The primary structure for GS is cyclo[VOLdFPVOLdFP], which is composed of a double-stranded antiparallel β -sheet connected by a pair of II' β -turns. The GS peptide is amphiphilic, with two polar side chains of Orn and two hydrophobic D-Phe rings as well as four hydrophobic Val and Leu side chains. A number of evidences exist that the major target of GS is the lipid bilayer of bacterial membranes. Several studies have been performed in order to understand the basis of its capacity to differentiate between bacterial and mammalian

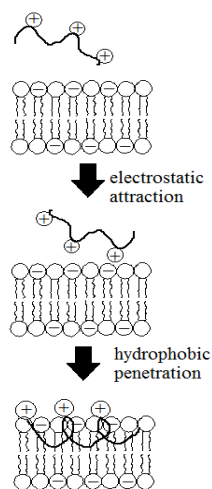


Figure 6. Different stages of peptide binding

cell membranes. One of the major differences between the lipid bilayers of mammalian and bacterial membranes is the presence of cholesterol in mammalian membranes. Previous studies performed by Abraham *et al.* used POPC with and without cholesterol to mimic the lipid composition of the mammalian membranes and bacterial membranes respectively. They performed the ITC experiments by injecting the lipid vesicles dispersion, with and without cholesterol respectively, into the GS solutions. Then the two binding isotherms obtained from the two ITC measurements were compared and analyzed. When cholesterol was present, a lower binding affinity and binding capacity were observed, indicating that cholesterol reduces the binding of peptide and membranes. Here, a similar ITC experiment was performed between the lipid vesicles and GS peptide solutions in order to develop in house capability for the study of lipid-peptide interactions, and also further illustrate how changes in lipid compositions, such as the incorporation of small molecules like cholesterol, affect the thermodynamics of the binding process.

Experimental methods

Large unilamellar vesicles (LUV) with 100 nm diameters were prepared as previously described in *lipid vesicle preparation*. POPC lipids were acquired from Avanti Polar Lipids, Alabaster, Alabama, USA. Lipid vesicles containing different percentage of cholesterol (0%, 20% and 40%) were prepared by co-dissolving POPC and cholesterol (Molar ratio 10:0, 10:2 and 10:4) in chloroform. All ITC measurements were performed using a high-sensitivity MicroCal ITC₂₀₀ (GE Healthcare) instrument. Titration experiments were performed by injecting 2 μ L of lipid vesicle solutions with a POPC concentration of 13.2mM – 26.3mM into the sample cell which contained 280 μ L of 50 μ M – 150 μ M GS solutions. Each injection produced a positive heat flow, indicating the binding of GS to lipid was endothermic and entropy-driven. Control experiments were performed by injecting the lipid vesicle solutions into water to determine the heat of dilution, which will then be subtracted from the heat of binding. The data obtained from the ITC measurement were fit to a one-site binding model in the Origin program. Three binding parameter including enthalpy change (ΔH), binding affinity (K_a), and binding stoichiometry (N) could be well resolved under these experimental conditions. The free energy of the binding, ΔG , can be calculated using the equation $\Delta G = -RT\ln(K_a)$. The entropy change for the binding can be obtained from the equation $\Delta S = (\Delta H - \Delta G)/T$.

Results and discussion

Figure 7 illustrates an ITC experiment in which 2 μ L \times 20 aliquots of POPC lipid vesicles containing 40% of cholesterol (19.7 mM) were repeatedly injected into the

sample cell containing 50 μM of GS. The upper panel displays the raw data obtained from the titration. Each injection produced an endothermic heat flow which decreases as a function of the number of POPC injections owing to the peptide concentration in the sample cell progressively decreasing. After ~ 10 injections, saturation occurred since there was almost no heat change observed, indicating that all of the peptide present in the sample cell had been bounded to the lipid vesicles. A control experiment was performed by injecting the same lipid vesicles solutions (40% cholesterol, 19.7 mM) into

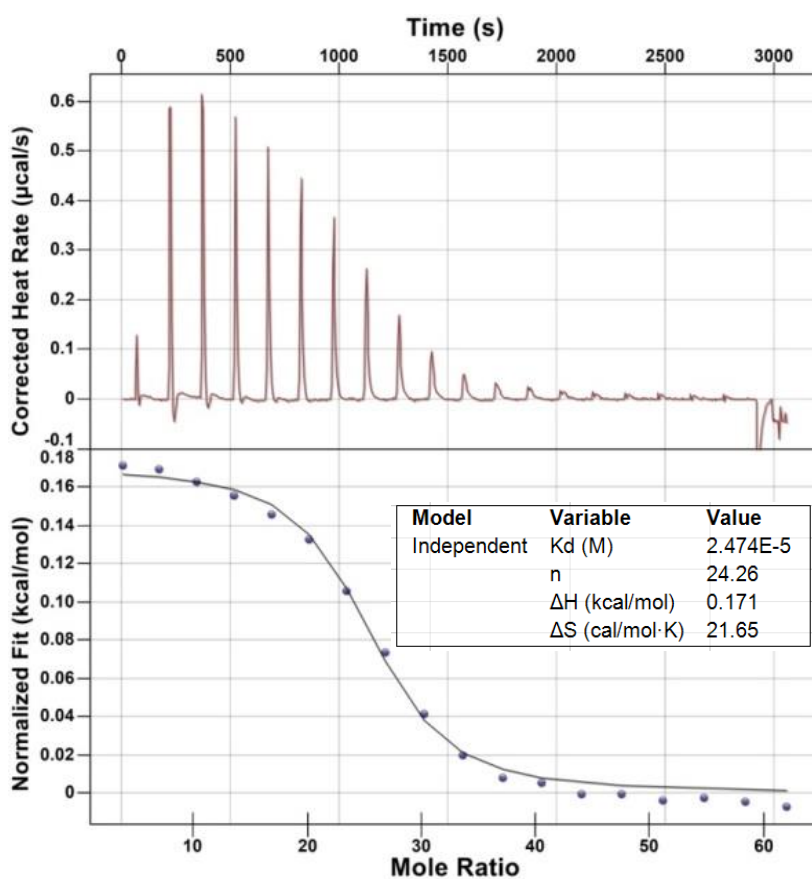


Figure 7. ITC experimental data at 25 °C. $20 \times 2 \mu\text{L}$ of 19.7 mM POPC/Cholesterol (10:4) was injected into 280 μL sample cell containing 50 μM GS. Data analysis was performed using Origin with built-in curve fitting models

water to determine the heat of the dilution, which was subtracted from the heat of binding. After that, a binding isotherm (Figure 7, lower panel) was generated from the corrected heat of binding and was fit into a one-site binding model. The ITC data analysis was performed using Origin with built-in curve fitting models. The c-value for the binding isotherm was 49, which is in the range of 20 to 100. Here, the three binding parameters could be well resolved. The ΔS was found to be 22 cal/mol·K and ΔH was 0.171 kJ/mol, which indicates the binding of GS to POPC is an entropy driven process with a positive ΔS counteracted with a positive ΔH . This result is consistent with the result obtained by Abraham *et. al* using the lipid vesicle with a diameter of 200 nm, although the values of the thermodynamic parameters are not the same owing to the difference in the vesicle size.

In addition, the ITC data analysis can also be performed manually using a series of equations.³⁶ The enthalpy of binding ΔH^0 can be calculated according to:

$$\Delta H^0 = \frac{\sum_i \delta h_i}{c_0^{\text{pep}} V_{\text{cell}}} \quad (2)$$

where δh_i is the heat of injection (heat of dilution subtracted), c_0^{pep} is the total peptide concentration within the calorimeter cell, and V_{cell} is the cell volume. In this case, δh_i was obtained by integrating each peak in the ITC raw data using Origin 8.5.1 (without built-in curve fitting models). c_0^{pep} was equal to 50 μM and V_{cell} was equal to 250 μL (30 μL of dead volume subtracted). Using equation (2), the value of ΔH^0 can be calculated which was equal to 3.9 kcal/mol. Here, ΔH^0 represents the heat absorbed per mole of peptide. However, when analyzing the data using Origin with built-in curve fitting models, ΔH represents heat absorbed per mole of injectant. Other thermodynamic

parameters can be found using Langmuir adsorption isotherm, which is mathematically equivalent to the “chemical” equilibrium. The Langmuir binding isotherm can be written as:

$$\frac{\theta}{1-\theta} = Kc_f \quad (3)$$

where $\theta = N \frac{c_{p,b}}{c_L}$ is the mole fraction of occupied binding sites. This binding model assumes that there are limited numbers of binding sites in the membrane and each binding site is made up of N energetically equivalent and noninteracting lipid molecules. In other words, one peptide (P) “reacts” with a cluster of N lipid (L) to form a PL_N complex. c_f is the concentration of free peptide. Based on equation (3), the binding isotherm can be derived from lipid-to-peptide titration according to the following equations. After i injections, the fraction of peptide $X_p^{(i)}$ bound to lipid vesicles is given by:

$$X_p^{(i)} = \frac{n_{p,b}^{(i)}}{n_{pep}^0} = \frac{\sum_{k=1}^i \delta h_k}{\sum_i \delta h_i} \quad (4)$$

where $n_{p,b}^{(i)}$ is the moles of bound peptide after i injections, n_{pep}^0 is the total moles of peptide in the sample cell, and $\sum_{k=1}^i \delta h_k$ is the sum of the first k reaction heats. The concentration of peptide remaining free in solution, $c_f^{(i)}$, is given by:

$$c_f^{(i)} = f_{dil}^{(i)} c_{pep}^{(0)} (1 - X_p^{(i)}) \quad (5)$$

where $f_{dil}^{(i)}$ is the dilution factor which takes into account the increase in volume due to vesicle injection and is defined as:

$$f_{dil}^{(i)} = \left(\frac{V_{cell}}{V_{cell} + V_{inj}} \right)^i \approx \left(\frac{V_{cell}}{V_{cell} + iV_{inj}} \right) \quad (6)$$

where V_{inj} is the injected volume per injection step ($V_{inj} / V_{cell} \ll 1$). The degree of peptide binding $X_b^{(i)}$ is defined as the mole ratio of bound peptide per lipid and is given by:

$$X_b^{(i)} = \frac{n_{psp,b}^{(i)}}{n_L^{(i)}} = X_P^{(i)} \frac{c_{psp}^0 V_{cell}}{i V_{inj} c_L^0} \quad (7)$$

where c_L^0 is the concentration of the lipid stock solution in the injection syringe. A plot of $X_b^{(i)}$ versus $c_f^{(i)}$ finally yields the desired binding isotherm, that is:

$$X_b^{(i)} = \frac{B_{max} K_c c_f^{(i)}}{1 + K_c c_f^{(i)}} \quad (8)$$

Using equation (8), the binding constant K_c and maximal binding capacity B_{max} can be obtained by plotting $X_b^{(i)}$ vs. c_f and fitting the data using Origin 8.5.1 (Figure 8). The maximal binding capacity of the lipid vesicle, B_{max} , is reciprocal to the binding stoichiometry, N ($B_{max} = 1/N$), which is the moles of bound peptide per moles of the total lipid. If we assume that each lipid vesicle is composed of the same number of lipid molecules, then B_{max} would be proportional to the number of peptide molecules bound per lipid vesicle. From these thermodynamic parameters, the free energy of binding, ΔG can be calculated using the standard relation:

$$\Delta G = -RT \ln(K_c) \quad (9)$$

and the binding reaction entropy ΔS can be calculated using the equation:

$$\Delta S = \frac{\Delta H - \Delta G}{T} \quad (10)$$

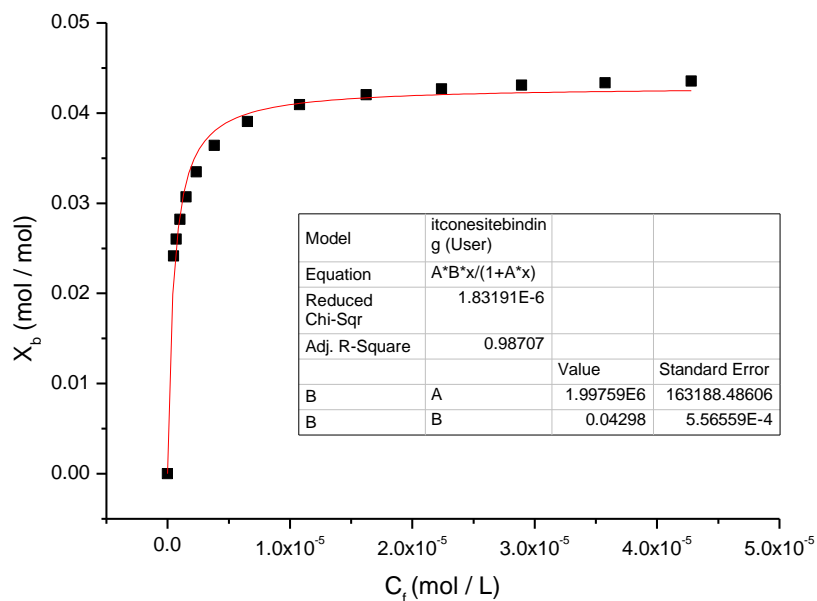


Figure 8. Binding isotherm for the binding of GS to lipid vesicles containing 40% of cholesterol derived from the ITC measurement at 25 °C. Data analysis was performed using Origin with built-in curve fitting models.

Table 1. Thermodynamic parameters for the binding of GS to lipid vesicles containing 40% of cholesterol

Thermodynamic parameters	Using Origin with built-in curve fitting models	Using Origin without built-in curve fitting models
K_d (10^{-5} M)	2.5 ± 0.8	1.2
N (mol/mol)	24.3 ± 0.6	23.3
ΔH (kcal/mol)	0.171 ± 0.006	0.157
ΔS (cal/mol K)	21.6	23.1
ΔG (kcal/mol)	-6.28	-6.73
K_a (10^4 M $^{-1}$)	4.0	8.6 ± 0.7
B_{max} (mol/mol)	0.0412	0.0430 ± 0.0005

Table 1 summarizes the thermodynamic parameters derived from the one-site binding model, using the software and equations, respectively. It can be seen that the binding stoichiometry (or maximal binding capacity) and binding enthalpy did not change too much when comparing the data obtained from the software and that from the equations. When fitting the data using Origin with built-in curve fitting models, the binding stoichiometry N was found to be 24.3 ± 0.6 and the binding enthalpy ΔH was found to be 0.171 ± 0.006 kcal/mol, whereas when fitting the data using Origin 8.5.1 without built-in curve fitting models, the binding stoichiometry N was found to be 23.3 and the binding enthalpy was found to be 0.157 kcal/mol. This suggests that the values of N and ΔH measured from the ITC were pretty reliable as can be seen that the values obtained using different fitting methods were relatively close. Also can be seen from Table 1 is that the errors of the measurement for N and ΔH were relatively low. However, for binding affinity K_a (or dissociation constant K_d), the error of the measurement were fairly high and there was a big difference between the value obtained from Origin with and without built-in curve fitting models. The possible source of error is that the c value in this case is not high enough to obtain an accurate measurement for K_a . Owing to the large uncertainty in K_a , all of the ITC data analysis in the following chapter were performed using both of the two curve fitting methods.

The effects of cholesterol on the binding of GS to lipid vesicles has been investigated by performing the three parallel ITC experiments using lipid vesicles containing 0%, 20% and 40% cholesterol. The results are displayed in Figure 9, Figure 12 and Table 2. All of the three binding isotherms were fit to a one-site binding model.

POPC+Chol (0% 20% 40%) to Gramicidin S

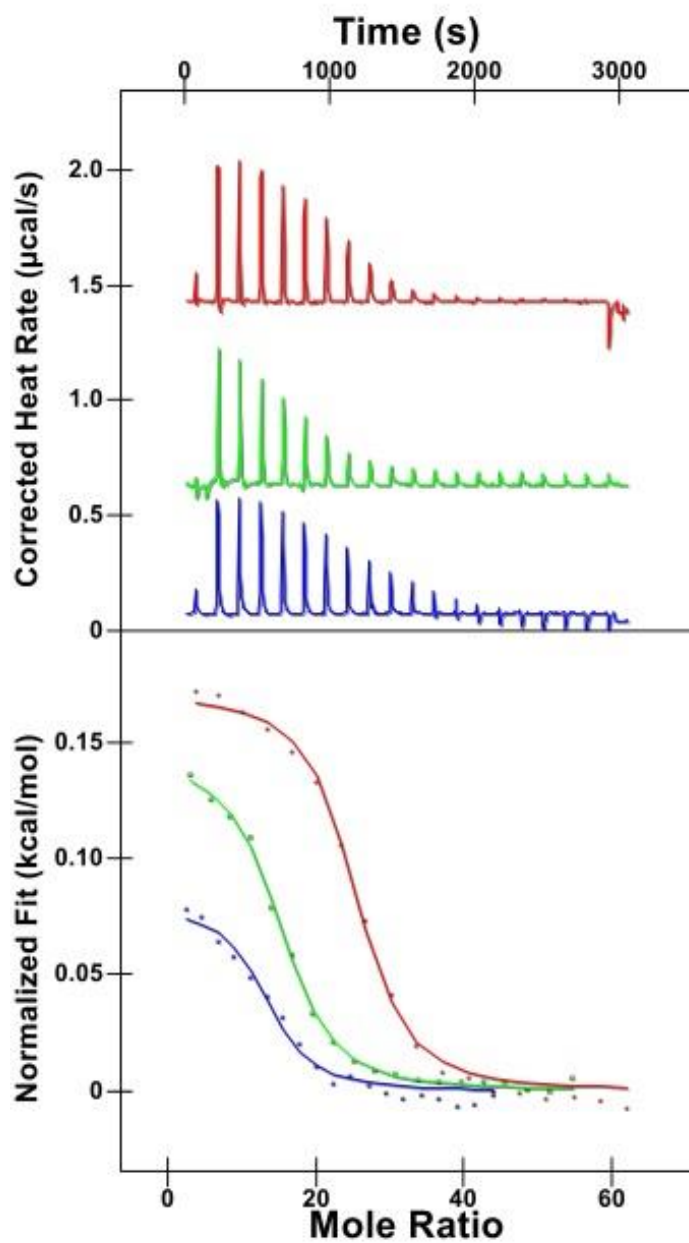


Figure 9. ITC experimental data of POPC LUV containing various amounts of cholesterol injected into GS. (Red: 40%, Green: 20% and Blue: 0%). Data analysis was performed using Origin with built-in curve fitting models.

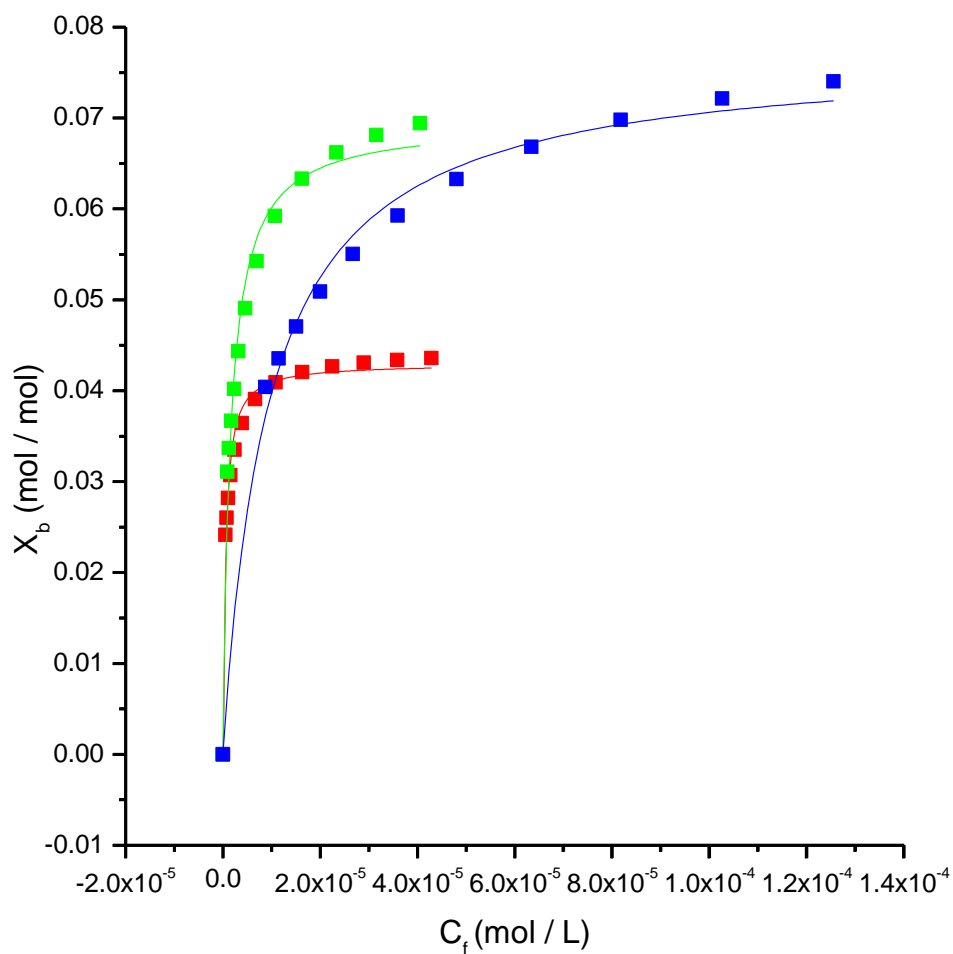


Figure 10. Binding isotherms for the binding of GS to lipid vesicles containing various amounts of cholesterol derived from the ITC measurement at 25 °C (Red: 40%, Green: 20% and Blue: 0%). Data analysis was performed using Origin without built-in curve fitting models.

Table 2. Thermodynamic parameters for the binding between GS and POPC LUV containing various amounts of cholesterol obtained using Origin with (upper panel) and without (lower panel) built-in curve fitting models respectively.

	Thermodynamic parameters	POPC +0%Chol	POPC +20%Chol	POPC +40%Chol
Using Origin with built-in curve fitting models	K_d ($10^{-4}M$)	1.1 \pm 0.7	0.44 \pm 0.09	0.25 \pm 0.08
	N	13.1 \pm 1.0	14.7 \pm 0.4	24.3 \pm 0.6
	ΔH (kcal/mol)	0.079 \pm 0.009	0.143 \pm 0.005	0.171 \pm 0.006
	ΔS (cal/mol K)	18.3	20.4	21.6
	ΔG (kcal/mol)	-5.38	-5.95	-6.28
	K_a ($10^4 M^{-1}$)	0.87	2.3	4.0
	B_{max} (mol/mol)	0.0763	0.0680	0.0412
Using Origin without built-in curve fitting models	K_d ($10^{-4}M$)	1.2	0.23	0.12
	N	13.0	14.4	23.3
	ΔH (kcal/mol)	0.082	0.125	0.157
	ΔS (cal/mol K)	18.2	21.7	23.1
	ΔG (kcal/mol)	-5.33	-6.34	-6.73
	K_a ($10^4 M^{-1}$)	0.81 \pm 0.05	4.4 \pm 0.4	8.6 \pm 0.7
	B_{max} (mol/mol)	0.0773 \pm 0.0010	0.0695 \pm 0.0010	0.0430 \pm 0.0005

The results revealed that as the percentage of cholesterol increases, the binding stoichiometry (N) increases as well, indicating the binding capacity B_{\max} decreases. This is consistent with the previous results shown by Abraham *et al.*, which indicates that cholesterol can reduce the binding of GS to POPC lipid vesicles owing to restricted flexibility of the tightly packed hydrocarbon chains. Also, with increasing cholesterol content, both of the change in enthalpy and entropy of the binding process become greater. The binding of GS to lipid bilayer is a complex process that includes (i) the conformational changes in the peptide (ii) displacement of water molecules from both peptide and membrane surfaces (iii) perturbation of the lipid membrane structure as a result of the peptide insertion.³⁷ Each of these processes would contribute to the ΔH and ΔS measured. Studies have shown that there is an increase in β -sheet content when GS is transferred from solution into lipid bilayers, but the heat change of this process is relatively small.²⁶ In fact, (ii) and (iii) are two major factors that contribute to the

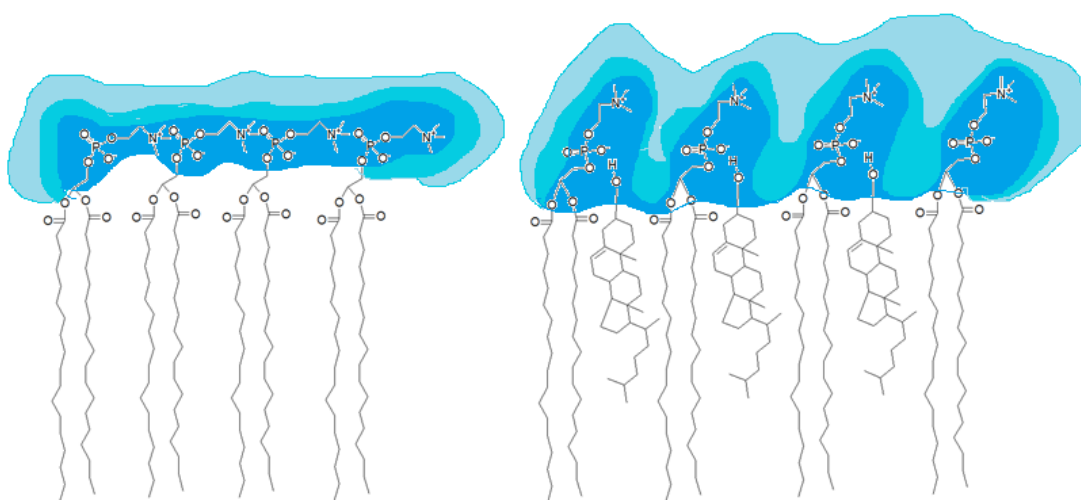


Figure 11. Lipid bilayer without and with cholesterol (Blue: hydration layer)

positive ΔH and ΔS values.³⁷ It is known that cholesterol can change the conformation of the lipid headgroup and create more space between lipid molecules since the $-OH$ group of cholesterol can form hydrogen bond with the phosphate group of a phospholipid.³⁸ As a result, it is possible that cholesterol can promote retention of a greater number of water molecules near lipid headgroups thus increasing the degree of hydration (Figure 11). Therefore, the ΔH of GS binding increases with an increase in cholesterol content since more energy is required to break the hydrogen bonds between water molecules and lipid headgroups. Additionally, the release of the ordered water molecules would result in an increase in entropy change since lipid bilayer with higher cholesterol content would release greater number of water molecules from its hydration layer, causing greater entropy change. Another factor that contributes to the positive ΔH and ΔS values is the perturbation of lipid bilayer structure. The positive ΔH component may originate from the peptide-induced increase of the bilayer area against surface tension to allow for peptide insertion.³⁷ It is proposed that incorporation of cholesterol in lipid bilayer results in increased cohesion and higher ordered hydrocarbon chains, which requires more work or energy to separate the acyl chains to allow for peptide insertion.²⁶ The increase in the area of the membrane upon binding also causes an increase in entropy owing to the disordering of lipid acyl chains.

Conclusions

The thermodynamics of the binding of GS to lipid vesicles vary with different lipid compositions. With increasing cholesterol content, the binding capacity of lipid vesicle for GS decreases, which is caused by the more restricted flexibility of the tightly

packed hydrocarbon chains after the incorporation of cholesterol. Also, as cholesterol content becomes greater, there is an increase in both enthalpy change and entropy change. Several factors that might be responsible for the change in enthalpy and entropy upon binding, including the change of the peptide conformation after its binding to the membrane; the dehydration of the peptides and the membrane surfaces; and the perturbation of the lipid membrane structure as a result of peptide insertion. Among these factors that might contribute to the changes in entropy and enthalpy, the dehydration process plays an important role and might be the major factor that causes the changes in the thermodynamic parameters after cholesterol has been incorporated. The increase in ΔH and ΔS values as a result of increasing cholesterol content might originate from the higher degree of hydration in lipid vesicles which have cholesterol included. These ITC results might help us understand the mechanisms of GS being able to differentiate between bacterial cell membranes and mammalian cell membranes.

CHAPTER IV

EFFECTS OF GRAMICIDIN A ON THE BINDING OF GRAMICIDIN S TO LIPID

BILAYERS STUDIED BY ISOTHERMAL TITRATION CALORIMETRY*

Introduction

Gramicidin A (GA) is a naturally occurring pentadecapeptide from *Bacillus brevis*. NMR studies revealed that when GA is bound to lipid membranes, an ion channel could be formed by head-to-head dimerization of two GA monomers, each in a single stranded helical conformation. Other conformation like the double helices may coexist with the head-to-head dimer.

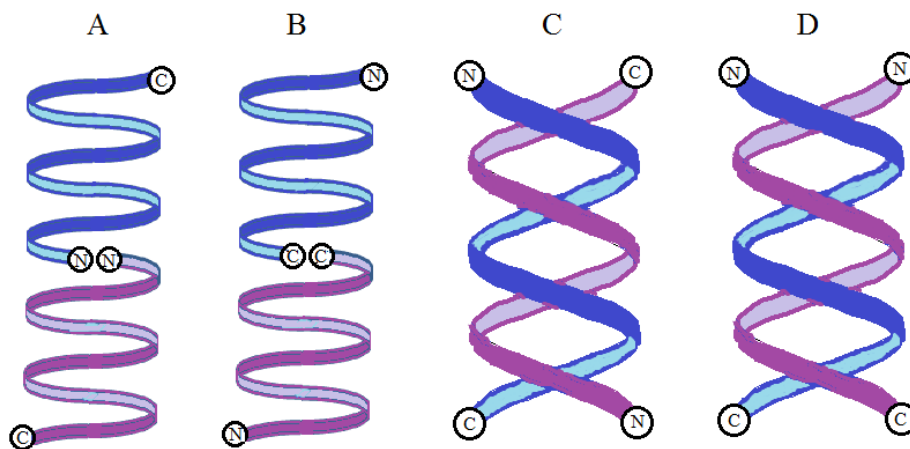


Figure 12. Different conformations of Gramicidin A (A: N-terminal to N-terminal head-to-head dimer; B: C-terminal to C-terminal head-to-head dimer; C: antiparallel double helice; and D: parallel double helice)

* Part of the data reported in this chapter is reprinted with permission from “Elucidation of conformer preferences for a hydrophobic antimicrobial peptide by vesicle capture-freeze-drying: a preparatory method coupled to ion mobility-mass spectrometry” by Patrick, J. W.; Gamez, R. C.; Russell, D. H, **2015**. *Anal Chem*, 87, 578-583, Copyright 2014 by American Chemical Society.

When GA is dissolved in organic solvent, such as methanol and ethanol, the GA dimers predominantly adopt double-stranded helices. Previous IM-MS by *Chen et al.* has shown that there is equilibrium between different conformations of GA dimer as well as GA monomer.³⁹ The monomerization kinetics and equilibrium abundances of the dimer ions depend upon solvent polarity. The kinetics of monomerization is slower for the longer chain alcohols. When comparing the three organic solvents such as ethanol, propanol, and isobutanol, the rate of monomerization of GA was slowest when GA was dissolved in isobutanol since it has the longest chain.

The conformation of GA can be influenced by the lipid composition and properties. Previous studies have demonstrated that IM-MS is capable of probing the membrane-bound structure of GA and the conformer preferences of GA dimer is highly dependent on the lipid environment.²³ Factors such as the acyl chain length and extent of acyl chain unsaturation will affect the conformer preference of GA in the membrane. The IM-MS studies of GA conformers in membrane require a sample preparation method VCFD (vesicle-capture-freeze-drying), which has been discussed before. Here, isobutanol was selected as the solvent to release the GA molecule from the lipid vesicle in order for it to be ionized by electrospray ionization. The purpose of using isobutanol as the solvent is to slow down the process of monomerization of GA in order to help preserve its original conformer preferences in the membrane. Using this method, different conformations of GA dimers can be resolved from the collision cross section (CCS) profiles (Figure 13). There are three major conformations of GA dimer observed:

single-stranded head-to-head dimers (SSHH, CCS = 673 Å²), antiparallel double helices (ADH, CCS = 679 Å²) and parallel double helices (PDH, CCS = 725 Å²). The results reveal that the conformational distribution of GA dimer is sensitive to the physical properties of the lipid composing the bilayer *i.e.* acyl chain length and degree of unsaturation. This suggests that to some extent, the membrane-bound conformations of GA dimers can be preserved when transferred from solution phase into the gas-phase.

Although IM-MS is capable of probing the structural changes of GA when it is incorporated into different lipid environment, it cannot provide information regarding how GA interacts with the lipid. For example, how does the insertion or binding of GA

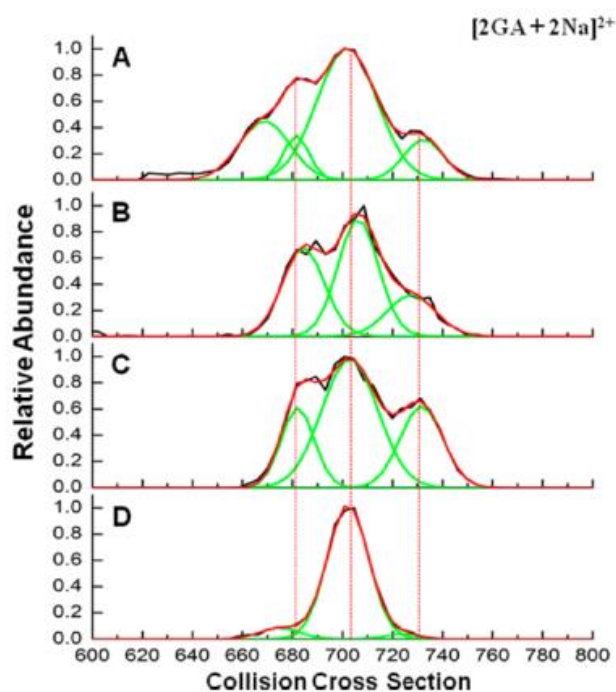


Figure 13. CCS profiles of GA $[2 M + 2 Na]^{2+}$ incorporated in 100 nm lipid vesicles formed using (A) DLPC (12:0 PC) (B) DMPC (14:0 PC) (C) POPC (16:0, 18:1 PC) (D) DEPC (22:1 PC)

affects the structure and properties of the surrounding lipids? And what is the location of GA molecules within the lipid bilayer? In order to answer these questions, we coupled IM-MS with ITC to better elucidate the interaction between GA and lipid bilayers. Chapter III discusses the effects of cholesterol on the binding process of GS to lipid vesicles. Since the thermodynamics of the binding depends upon lipid compositions, it is possible to incorporate GA into the bilayer to study how the presence of GA affects the binding of GS, which would provide information on how insertion of GA affects the physicochemical properties of the lipid. The effects of amino acid modifications of GA will also be investigated using this method. Molecular dynamic simulation has shown that deomylation of GA would cause a higher abundance of double helices and a lower abundance of head-to-head dimer.⁴⁰ This can be explained by the fact that the head-to-head dimer will be destabilized by deomylation since the introduction of two positive charges on N-termini cause electrostatic repulsion between the two positive charges that are in close proximity. For double helices, however, the two positively charged N-terminus could be stabilized by the solvation of water and lipid headgroup when GA is located on the water-lipid interface. Similar results were obtained from IM-MS studies using VCFD method, which has shown that deomylation of the N-terminus of GA caused a shift to higher abundance of double helices.²³ In this chapter, we would discuss the effects of deomylation on GA-lipid interactions using ITC in combination with IM-MS.

Experimental methods

GA peptide powder was obtained from Sigma-Aldrich St. Louis, Mo, USA and was used without further purification. POPC lipid was obtained from Avanti Polar Lipids, Alabaster, Alabama, USA. Deformylated GA was prepared by mixing 3.2 mg/ml GA in methanol with 2.0 M hydrochloric acid for 2 h followed by lyophilization to yield a dry powder.²³ The GA peptide and deformylated GA peptide were dissolved in ethanol respectively and combined with POPC lipid in chloroform at a molar ratio of 100:1, dried under N₂ gas until solvent was removed. Lipid vesicles loaded with GA and deformylated GA was then made as previously described in *lipid vesicle preparation*. After that, ITC experiment was performed between GS and lipid vesicle loaded with GA, as well as between GS and lipid vesicle loaded with deformylated GA. All ITC measurements were performed using a high-sensitivity MicroCal ITC₂₀₀ (GE Healthcare) instrument. Titration experiments were performed by injecting 20 × 2 μL of lipid vesicle solutions with a POPC concentration of 19.7 mM into the sample cell which contained 280 μL of 50 μM GS solutions. For both GA and deformylated GA, the ITC experiment was performed at the same lipid concentration and GS concentration. Control experiments were performed by injecting the lipid vesicle solutions into water to determine the heat of dilution, which will then be subtracted from the heat of binding. The data obtained from the ITC measurement were fit to a one-site binding model in the Origin program to obtain the thermodynamic parameters. The data obtained from lipid vesicles loaded with GA and deformylated GA can be compared to analyze the effects of deformylation.

Results and discussion

The ITC data (Figure 15) shows that incorporation of GA into the membrane has a significant effect on the binding of GS. After incorporation of GA, a decrease in ΔH , ΔS and binding capacity were observed in the ITC measurement, indicating that the insertion or binding of GA may impact the hydration layer of the membrane surface as well as the lipid acyl chains. As has been discussed above, the changes in enthalpy and entropy primarily originate from two processes: the displacement of water from the peptide and membrane surface, and the perturbation of the lipid acyl hydrocarbon chains. NMR studies suggest that GA dimer are located in the hydrophobic core region of the lipid bilayers,¹⁷ thus the perturbation of the lipid chains is probably a major factor. Molecular dynamic studies showed that owing to the hydrophobic mismatch between the GA and surrounding lipid bilayer, the lipid chain conformation becomes disordered and the hydrophobic thickness of the bilayer can increase or decrease to fit the length of the hydrophobic core region of the GA dimer.⁴¹ As a result, there would be less energy required to separate the lipid acyl chains in order to allow the insertion of GS, thus a lower ΔH value was observed from the ITC experiment.

When deformed GA was incorporated into the lipid bilayers, the effects on the binding isotherms are different as opposed to GA (Figure 15). De groot *et al.* has reported that deformation of GA caused a higher abundance of double helices and a lower abundance of head-to-head dimer, which can be explained by the fact that in parallel double helices, the two positively charged N-termini are located on the interface of membrane surface and hydration layer and thus can be fully solvated by the polar

headgroup and water. However, the head-to-head dimer will be destabilized by deformylation since the introduction of two positive charges on N-termini cause electrostatic repulsion between the two positive charges that are in close proximity.⁴⁰ Similar results were obtained from CCS profiles of GA and deformylated GA in POPC lipid vesicles (Figure 14).²³ These results suggest that the location of GA and

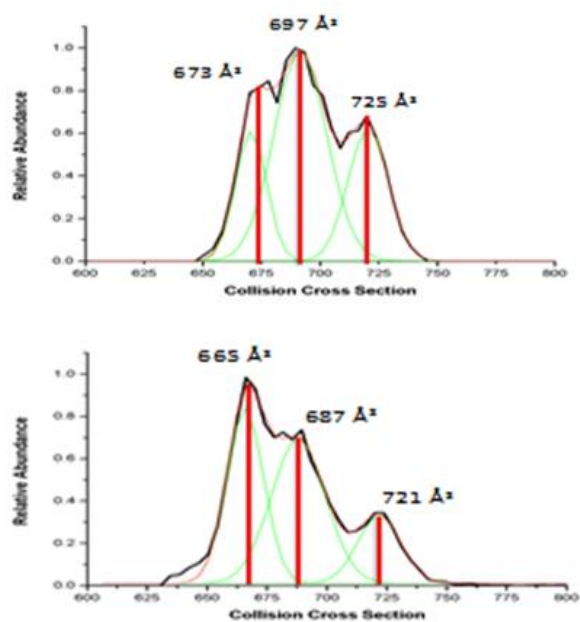


Figure 14. Collision cross section (CCS) profiles of GA (upper panel) and deformylated GA (lower panel) in POPC lipid vesicle

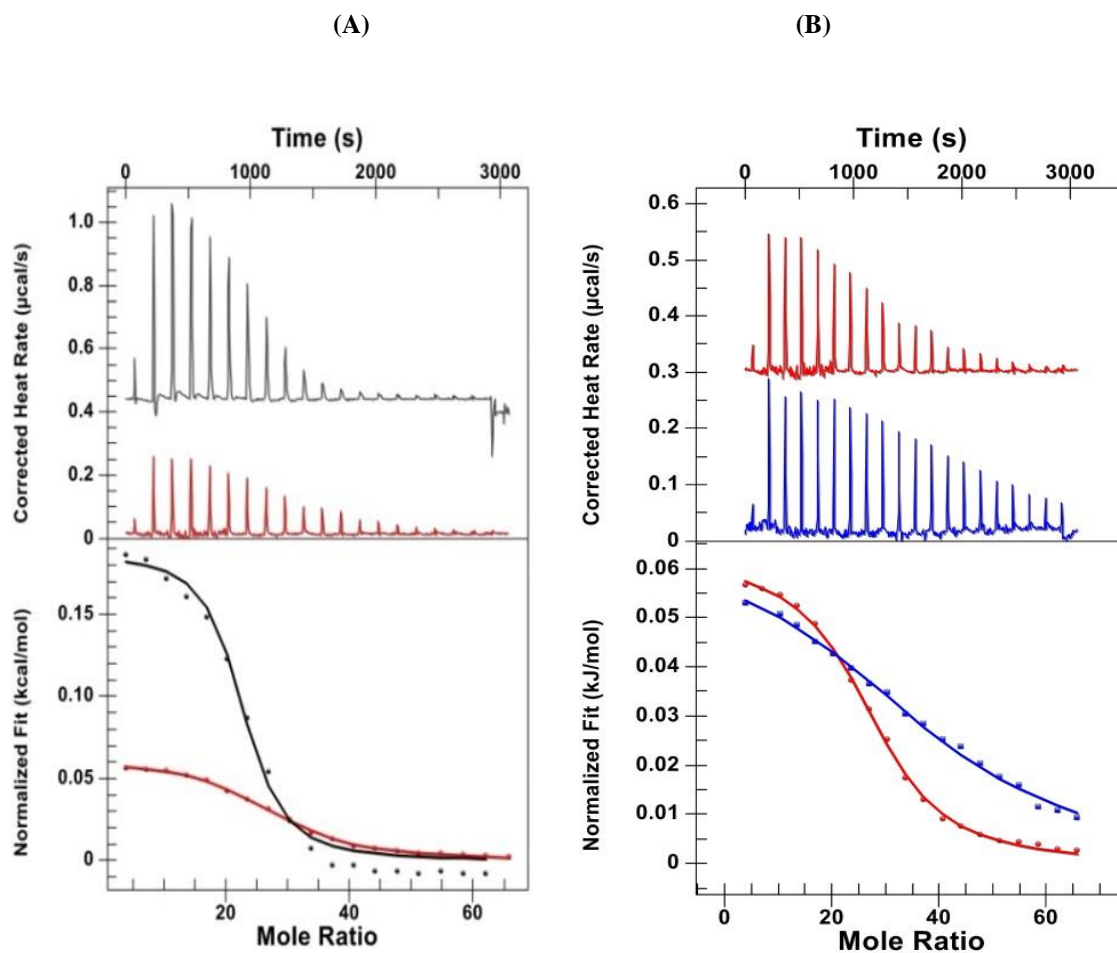


Figure 15. (A) ITC experimental data of POPC LUV with (red) and without (black) GA bound injected into GS solution. (B) ITC experimental data of POPC LUV with GA (red) / deformed GA (blue) bound injected into GS. Molar ratio between POPC and GA (deformed GA) was 100:1. The concentration of POPC lipid was 19.7 mM. The thermodynamic parameters for all binding isotherms are shown in Table 3.

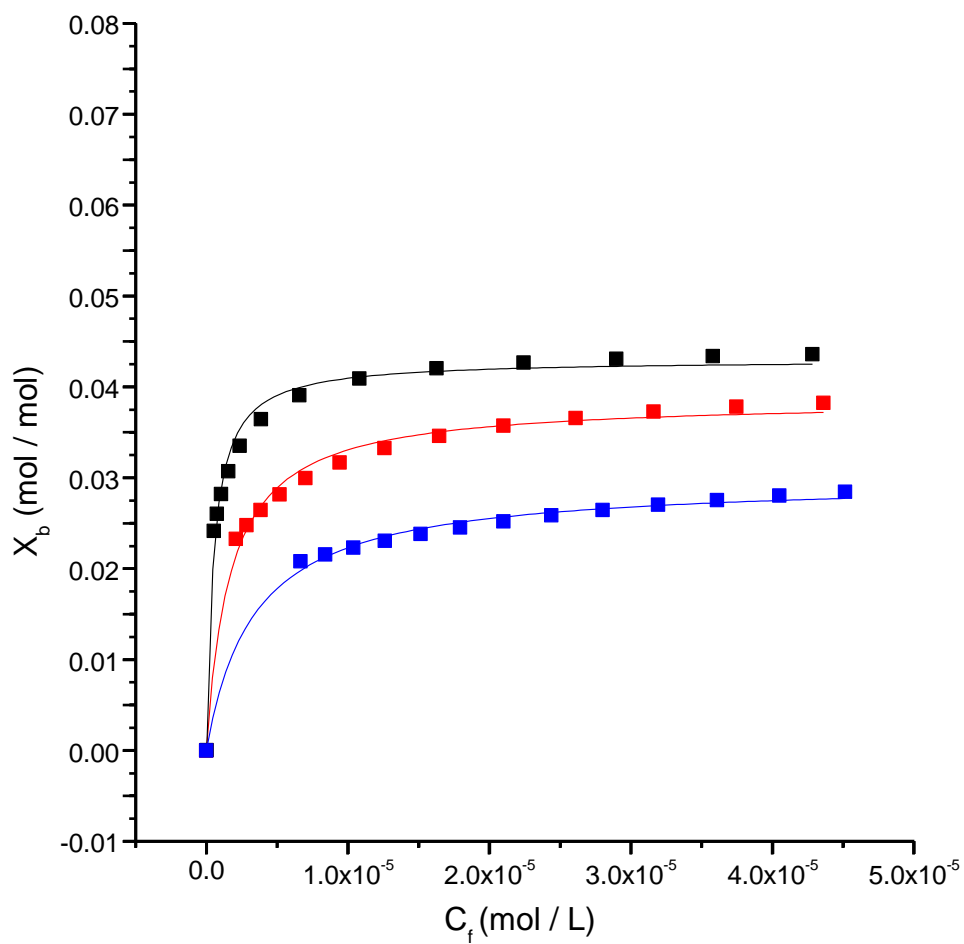


Figure 16. Binding isotherms for the binding of GS to lipid vesicles with GA (red) and dGA (blue) bound as well as no GA/deformylated GA bound (control: black). Data analysis was performed using Origin 8.5.1.

Table 3. Thermodynamic parameters for the binding between GS and POPC LUV with and without GA (deformylated GA)

	Thermodynamic parameters	POPC	POPC+GA	POPC+dGA
Using Origin with built-in curve fitting models	K_d (10^{-4} M)	0.25±0.08	0.97±0.10	4.2±0.8
	N	24.3±0.6	27.4±0.4	39.4±2.0
	ΔH (kcal/mol)	0.171±0.006	0.062±0.001	0.066±0.004
	ΔS (cal/mol K)	21.6	18.6	15.7
	ΔG (kcal/mol)	-6.28	-5.47	-4.61
	K_a (10^4 M ⁻¹)	4.0	1.0	0.24
	B_{max} (mol/mol)	0.0412	0.0364	0.0254
Using Origin without built-in curve fitting models	K_d (10^{-4} M)	0.12	0.43	1.1
	N	23.3	25.9	33.6
	ΔH (kcal/mol)	0.157	0.052	0.046
	ΔS (cal/mol K)	23.1	20.1	13.6
	ΔG (kcal/mol)	-6.73	-5.95	-4.02
	K_a (10^4 M ⁻¹)	8.6±0.7	2.3±0.2	0.88±0.07
	B_{max} (mol/mol)	0.0430±0.0005	0.0386±0.0005	0.0298±0.0004

deformylated GA are different in lipid bilayer. We hypothesized that GA is primarily located inside the lipid bilayer *i.e.* hydrophobic core or polar-nonpolar interface region to maximize the hydrophobic interaction between GA and lipid acyl chains, whereas the deformylated GA is primarily located on the lipid-water interface where two positive charges on the N-terminus could be solvated. This could explain why GA and deformylated GA affect the binding of GS differently. Owing to its proximity to the membrane surface, deformylated GA could affect the binding through two processes: changing the hydration layer of lipid membrane and changing the lipid acyl chain conformation. For GA, it would affect the binding primarily through changing the lipid acyl chain conformation because it has little effect on the membrane surface owing to its hydrophobic character. As can be seen from the ITC results (Figure 15), incorporation of GA weakens the binding of GS slightly while incorporation of deformylated GA strongly weakens the binding, with both a much lower K_a and B_{max} . This is probably caused by the two positive charges of the N-terminus of deformylated GA being exposed to the surface of the membrane, which would reduce the electrostatic attractions between the positively charged GS peptide and the negative charge on the headgroup of the lipid. On the other hand, the positive charges on GA introduced by deformylation could also cause electrostatic repulsion with the positively charged GS, which further reduce the binding of GS. Also, a much smaller ΔS value was observed for lipid vesicle loaded with deformylated GA as opposed to GA, which could be explained by the fact that less water molecules are retained on the surface of lipid membrane loaded with deformylated GA. The extra charges on the membrane surface introduced by the deformylated GA would

perturb the hydration layer and cause it to become thinner. Therefore, when GS was inserted into the membrane, a lower number of water molecules would be released from the membrane surface, causing a lower entropy gain for the system.

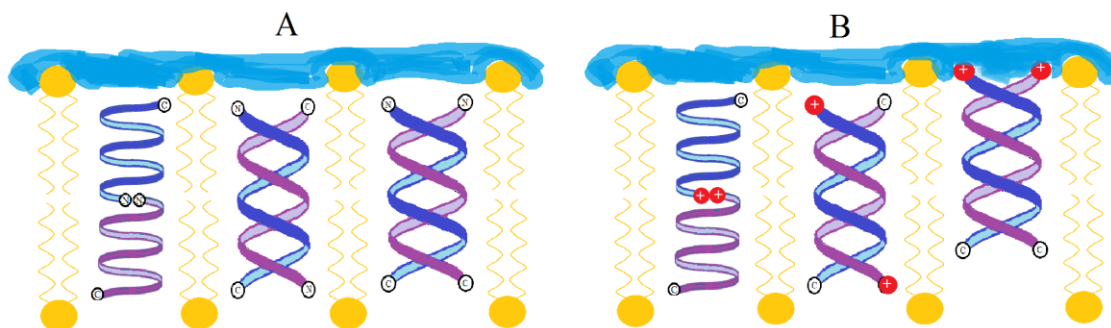


Figure 17. Effects of N-terminus deformylation on GA-lipid interactions ((A) Before deformylation; (B) After deformylation; Blue: hydration layer)

Conclusions

The thermodynamics of the GS binding to lipid vesicles depends upon lipid compositions and thus can be utilized to study the effects of the incorporation of GA as well as deformed GA. Therefore, when ITC results are combined with IM-MS results, information regarding how insertion of GA affects the structure and properties of the surrounding lipids and how deformation of N-terminus affects the structure and conformation of GA and thus affects the interaction of GA and lipid bilayer could be investigated. It was shown that GA could affect the binding of GS mainly through interacting with the lipid acyl chains and therefore make the conformation of the acyl chains more disordered. This would cause a lower ΔH in the binding process of GS to lipid vesicles owing to less energy needed to separate the lipid acyl chains with more disordered structures. When the ITC data of GS binding to lipid vesicles with GA and deformed GA are compared, there is a significant difference in the shape of the binding isotherms, indicating that deformation of GA N-terminus would affect GA-lipid interactions. The introduction of two positive charges on the N-terminus of GA would destabilize the SSSH conformation owing to the coulombic repulsion between the two charges that are in close proximity. The PDH conformation could be stabilized by interacting with the hydration layer as well as the lipid headgroup since it is located close to the surface of the membrane. As a result, deformed GA could affect the structure and properties of lipid acyl chains as well as the hydration layer on the membrane surface. When GS interacts with lipid vesicles incorporated with deformed GA, the positive charges of the N-terminus of GA will reduce the

coulombic attraction between GS and membrane, thus reducing the binding capacity and binding affinity of the lipid vesicles to GS. It was shown from the ITC data that a much weaker binding was observed for GS to lipid vesicles with deformed GA when compared with GA. GA, on the other hand, would not be able to affect the binding of GS through the hydration layer owing to its extremely hydrophobic character. Therefore, GA did not change the binding affinity and binding stoichiometry that much as opposed to deformed GA.

CHAPTER V

ION MOBILITY MASS SPECTROMETRY STUDIES OF CONFORMATIONAL CHANGES OF GRAMICIDIN A INDUCED BY THE BINDING OF GRAMICIDIN S

Introduction

It is known that the cyclic decapeptide Gramicidin S (GS) exhibits a broad spectrum of antibiotic activity against Gram-positive and Gram-negative bacteria and fungi. However, little is known about the mechanism of the interaction of GS with lipid model membrane systems.⁴² Considerable efforts have been directed at studying the relationship between the molecular structure and antibiotic activity of GS in order to elucidate the mechanism of its action. The purpose in understanding the mechanism is to develop GS derivatives of comparable or enhanced antibiotic activity.⁴²

Previous studies have shown that GS probably interacts primarily with the headgroup and polar/apolar interfacial regions of lipid bilayer model membranes. It has been proposed to induce the formation of pores in its membrane targets, a mechanistic feature common to many antibiotic peptides.⁴² There are several factors that may influence its interaction with the lipid bilayer, *i.e.*, the lipid-GS interactions are stronger in the liquid-crystalline than in the gel state. GS interacts more strongly with anionic as compared to zwitterionic phospholipid bilayers.⁴³ In addition, it was demonstrated that the lipid: peptide ratio may also play a role in mediating their interactions. ³⁴P NMR and X-ray diffraction studies indicated that GS at low concentration causes the thinning of phospholipid bilayers and can induce the formation of inverted nonlamellar cubic phases

in phospholipic dispersions at higher concentrations.⁴³ Other studies have shown that at physiologically relevant concentrations of GS (lipid/peptide ratios of 25:1), GS does not affect the lamellar phase preference of the zwitterionic lipids PC.⁴² However, when the lipid/peptide ratios are extremely low (<3:1), it can cause the total disruption of liquid-crystalline bilayers.⁴⁴

In this chapter, we would discuss a new method which utilizes IM-MS as an analytical tool and GA as a “reporter” peptide to study how changes in lipid/GS molar ratio affect their interactions. As has been discussed before, the conformer preferences of GA dimer depends upon lipid environment, which can be probed by IM-MS. So here, we incorporated GA into the lipid bilayers model system at the beginning, and then added various amounts of GS peptide to the membrane system to change the molar ratio between lipid and GS. If the binding of GS with lipid bilayer changes the lipid environment, *i.e.*, thinning of phospholipid bilayers or formation of inverted nonlamellar cubic phases, we will be able to observe a series of changes in the CCS profiles of GA dimer, since the conformational distribution of GA is sensitive to the lipid environment. In this way, we could get a better understanding about the mechanism of the interaction between GS and membrane using IM-MS.

Experimental methods

GA peptide powder was obtained from Sigma-Aldrich St. Louis, Mo, USA and was used without further purification. POPC lipid was obtained from Avanti Polar Lipids, Alabaster, Alabama, USA. The GA peptide was dissolved in ethanol and combined with POPC lipid in chloroform at a molar ratio of 100:1, dried under N₂ gas

until solvent was removed. Lipid vesicles loaded with GA were then made as previously described in *lipid vesicle preparation*. After the lipid vesicles loaded with GA were formed, it was split into 7 vials, with each vials having equal amount of lipid with GA. Then various amounts of GS solutions were added into each vial to make different lipid/GS ratios (From 132:1 to 132:12). The control had no GS solution added. All solutions were allowed to incubate at 4 °C overnight followed by freeze-dried using liquid nitrogen and a vacuum desiccator to remove water. After that, the samples were rehydrated with isobutanol for ESI-IM-MS analysis.²³

In this study, the IM-MS were acquired on a Water SynaptTM HDMS G2 mass spectrometer (Waters Corp., Milford, MA). Ions were formed by nano-ESI with a source temperature of ~100 °C. The capillary voltage applied to the ESI tips was 1.5-2 kV. The instrument was equipped with a traveling-wave ion mobility cell with 30 V wave height and 300 m/s wave velocity. Sampling one voltage and extraction cone voltage were set at 15 V and 4 V respectively. The data analysis for IM experiment was performed using MassLynx v4.1 software. The CCS values for GA dimers were obtained using calibration method described previously by Ruotolo *et al.*³² The doubly charged tryptic digest ions of cytochrome C and myoglobin were used as calibrants, and their CCS were obtained from collision cross section database generated by Clemmer and coworkers.³⁴

Results and discussions

Figure 18. shows the IM-MS results obtained from the samples described above that have different lipid/GS molar ratios. As can be seen from these results that the molar ratio of lipid/GS has significant effects on the conformer preferences of GA

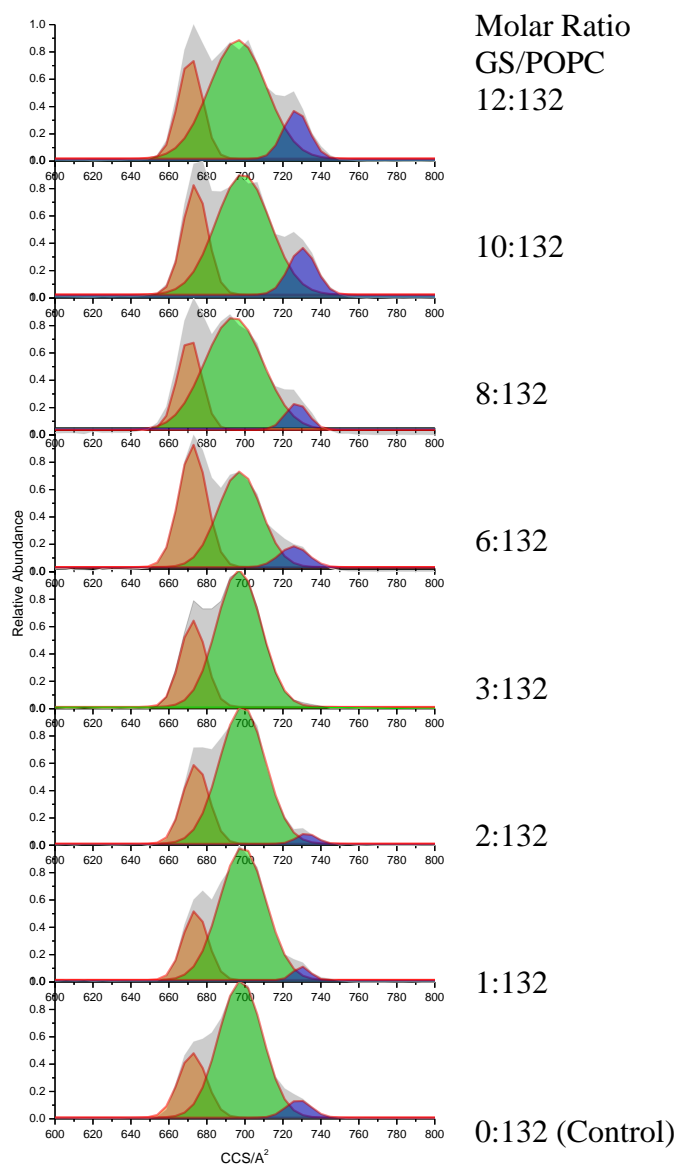


Figure 18. CCS profiles of GA dimer $[2 M + 2Na^+]$ in POPC lipid vesicles with various amounts of GS bound

dimer, which suggests that the binding of GS does depend upon the concentration of GS. Low concentration of GS and high concentration of GS would affect the lipid structure and properties differently, which can be seen from the IM-MS data that the CCS profiles differ a lot when the molar ratio increases from 1:132 to 12:132.

When the molar ratio is low (GS/lipid = 1:132 ~ 3:132), the CCS profiles of GA dimer only changes slightly when compared with the control (GS/lipid = 0:132). The most abundant conformers under low GS concentration is the ADH, with a slightly increase in the relative abundance of PDH and a slightly decrease in the relative abundance of SSHH as the concentration of GS goes up. When the molar ratio reaches 3:132, there is almost no SSHH observed from the IM-MS and only two conformers of GA dimers exist: PDH and ADH. Since previous studies have shown that GS does not affect the lamellar phase preference of the zwitterionic lipid POPC when the GS/lipid molar ratio is below 1:25 and that GS at low concentration only causes the thinning of phospholipid bilayers,^{43,44} it can be explained that these slight changes in the CCS profiles of GA dimer are probably just caused by the thinning of the POPC lipid vesicle bilayers. The decrease in the thickness of the lipid bilayer can no longer accommodate for the SSHH since its length is the longest among the three conformers. As a result, we could observe a shift from SSHH to PDH as we slightly increase the concentration of GS.

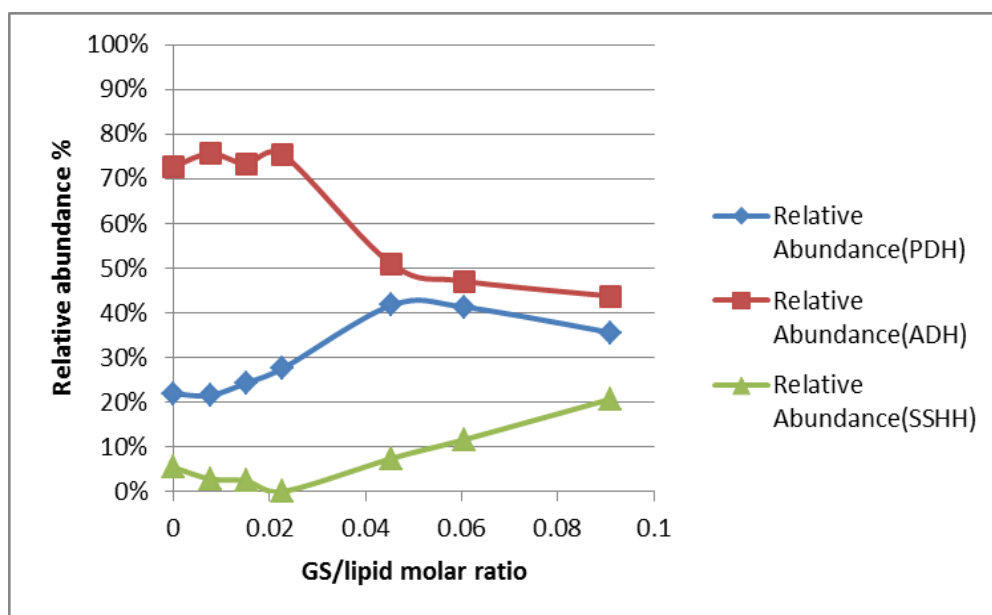


Figure 19. Plots of relative abundances of the three GA dimers as a function of GS/lipid molar ratios

However, when the peptide/lipid ratios are high, it can cause the total disruption of liquid-crystalline bilayers.⁴⁴ Studies have shown that high GS concentration could cause formation of inverted nonlamellar cubic phases.^{43,44} As can be seen from Figure 19, when the molar ratios of GS/lipid changes from 6:132 to 12:132, the conformational distribution of GA changes dramatically as compared with the control. The peak corresponding to the ADH conformers become much broader when the GS concentration is high, suggesting that there might be more than one conformer of ADH. Also, the relative abundances of PDH and SSHH increases as the GS concentration goes up, whereas the relative abundance of ADH decreases. As a result, when the GS concentration reaches the highest (GS/lipid = 12:132), the relative abundance of ADH is

not that dominant when compared with the control. These change might have been caused by the total disruption of the lipid bilayers at high GS concentration. The formation of inverted nonlamellar cubic phases in the lipid bilayers may induce a completely change in the conformational distribution of GA dimer, thus changing the relative abundances of each conformer as well as inducing the formation of new conformer.

Conclusions

The effects of GS binding to lipid bilayer are dependent on GS concentration or the molar ratio between GS and lipid. Previous studies using DSC, ³¹P NMR and X-ray diffraction has demonstrated that low concentration of GS only causes thinning of the phospholipid bilayers, whereas high concentration of GS could cause total disruption of the bilayer and induce the formation of inverted nonlamellar cubic phase in the lipid bilayers. Here, a novel method using IM-MS to probe the effects of changes in GS concentrations on the lipid environment has been described. This method uses GA as a “reporter” in the IM-MS experiment, and the changes in the CCS profiles of GA could provide information regarding how the lipid properties and structures change as a function of GS concentrations. It was shown that at low GS concentration, only slight change in CCS profiles of GA was observed, indicating the thinning of lipid bilayers caused by GS under low concentration condition. When the GS concentration is high, a significant change in CCS profiles of GA was observed, including the broadening of the peaks as well as a completely change in the relative abundances of the three conformers. This suggests that a total disruption of the bilayers occurs at high GS concentrations and

it might have induced the formation of inverted nonlamellar cubic phase in the lipid bilayers. This novel technique has many advantages over the traditional methods such as DSC, NMR and X-ray diffraction. First of all, we could use GA as a “reporter” to visualize what is happening inside the lipid bilayers, which is easy and straightforward compared with other techniques. Secondly, the amount of sample needed for the IM-MS experiment is very low. Lastly, this method does not require long data acquisition time and complicated data analysis, which is time consuming.

CHAPTER VI

SUMMARY

In this study, IM-MS coupled with ITC are utilized to understand the molecular mechanism of the interaction between GA and lipid bilayer model system as well as the interaction between GS and lipid bilayer model system. The experimental results from both the IM-MS and ITC provide valuable information regarding how insertion or binding of antimicrobial peptide GA and GS affects the lipid structures and properties, other information such as how modification of the N-terminus of GA affects its interaction with the lipid bilayers is also provided.

In the first part of the study, we were using ITC to study the thermodynamics of the binding between GS and lipid bilayers. Our results suggest that the thermodynamics of the binding process is highly dependent upon the lipid composition. Lipid bilayers with various amounts of cholesterol incorporated will result in binding isotherms with different thermodynamic parameters. The way that cholesterol affects the binding is probably through different processes, including the conformational changes in the peptide, the displacement of water molecules from peptide and membrane surfaces, as well as perturbation of the lipid membrane structure as a result of peptide insertion. Among these processes, cholesterol might influence the binding primarily through disturbing the lipid acyl chains and changing the membrane hydration layer.

Based on these results, we continued our research by incorporating GA into the lipid bilayer and study how the presence of GA affects the binding of GS to lipid bilayer

using ITC. At the same time, we modified the N-terminus of GA by deformylation, which introduced two positive charges on the N-terminus, and the deformylated GA was also incorporated into the membrane system in order to investigate the effects of deformylation on the interaction between GA and lipid bilayers. Our results showed that the introduction of two positive charges on the N-terminus of GA causes a much weaker binding between GS and lipid vesicles. This can be explained by the fact that the positive charges of deformylated GA reduce the coulombic attraction between GS and membrane owing to the charges located close to the surface of the membrane. This hypothesis can be further supported by the previous IM-MS results, which indicates that deformylation causes a shift from SSHH to PDH, since the N-terminus of PDH can be solvated by the lipid headgroup and hydration layer whereas the SSHH will be destabilized by the two positively charged N-termini that are in close proximity. Here, by combining ITC results and IM-MS results, we could not only obtain the structural information of GA or deformylated GA in the membrane, but also investigate how the presence of GA or deformylated GA affects the surrounding lipid.

In the last part, we used GA as a “reporter” to investigate how interaction with GS changes the structure and properties of lipid bilayer. The IM-MS data of GA in lipid vesicles treated with various amounts of GS has shown how conformer preferences of GA changes as a function of GS concentration, which further reveal how lipid structure and properties changes as a function of GS concentration. The data analysis is much easier and the results are much more straightforward when it is compared with traditional technique such as NMR and X-ray diffraction.

REFERENCES

- (1) Galdiero, S.; Falanga, A.; Cantisani, M.; Vitiello, M.; Morelli, G.; Galdiero, M. Peptide-lipid interactions: experiments and applications. *Int J Mol Sci* **2013**, *14*, 18758-18789.
- (2) Steiner, H.; Hultmark, D.; Engstrom, A.; Bennich, H.; Boman, H. G. Sequence and specificity of two antibacterial proteins involved in insect immunity. *Nature* **1981**, *292*, 246-248.
- (3) Bechinger, B. Structure and functions of channel-forming peptides: magainins, cecropins, melittin and alamethicin. *J Membr Biol* **1997**, *156*, 197-211.
- (4) Woolley, G. A.; Wallace, B. A. Model ion channels: gramicidin and alamethicin. *J Membr Biol* **1992**, *129*, 109-136.
- (5) Bechinger, B. The structure, dynamics and orientation of antimicrobial peptides in membranes by multidimensional solid-state NMR spectroscopy. *Biochim Biophys Acta* **1999**, *1462*, 157-183.
- (6) Falanga, A.; Tarallo, R.; Vitiello, G.; Vitiello, M.; Perillo, E.; Cantisani, M.; D'Errico, G.; Galdiero, M.; Galdiero, S. Biophysical characterization and membrane interaction of the two fusion loops of glycoprotein B from herpes simplex type I virus. *PLoS One* **2012**, *7*, e32186.
- (7) Vitiello, G.; Falanga, A.; Galdiero, M.; Marsh, D.; Galdiero, S.; D'Errico, G. Lipid composition modulates the interaction of peptides deriving from herpes simplex virus type I glycoproteins B and H with biomembranes. *Biochim Biophys Acta* **2011**, *1808*, 2517-2526.
- (8) Castano, S.; Desbat, B. Structure and orientation study of fusion peptide FP23 of gp41 from HIV-1 alone or inserted into various lipid membrane models (mono-, bi- and multibi-layers) by FT-IR spectroscopies and Brewster angle microscopy. *Biochim Biophys Acta* **2005**, *1715*, 81-95.
- (9) Sani, M. A.; Loudet, C.; Grobner, G.; Dufourc, E. J. Pro-apoptotic bax-alpha1 synthesis and evidence for beta-sheet to alpha-helix conformational change as triggered by negatively charged lipid membranes. *J Pept Sci* **2007**, *13*, 100-106.
- (10) D'Errico, G.; Ercole, C.; Lista, M.; Pizzo, E.; Falanga, A.; Galdiero, S.; Spadaccini, R.; Picone, D. Enforcing the positive charge of N-termini enhances membrane interaction and antitumor activity of bovine seminal ribonuclease. *Biochim Biophys Acta* **2011**, *1808*, 3007-3015.

- (11) Karle, I. L.; Perozzo, M. A.; Mishra, V. K.; Balaram, P. Crystal structure of the channel-forming polypeptide antimioebin in a membrane-mimetic environment. *Proc Natl Acad Sci U S A* **1998**, *95*, 5501-5504.
- (12) Bechinger, B.; Resende, J. M.; Aisenbrey, C. The structural and topological analysis of membrane-associated polypeptides by oriented solid-state NMR spectroscopy: established concepts and novel developments. *Biophys Chem* **2011**, *153*, 115-125.
- (13) Salnikov, E.; Rosay, M.; Pawsey, S.; Ouari, O.; Tordo, P.; Bechinger, B. Solid-state NMR spectroscopy of oriented membrane polypeptides at 100 K with signal enhancement by dynamic nuclear polarization. *J Am Chem Soc* **2010**, *132*, 5940-5941.
- (14) La Rocca, P.; Biggin, P. C.; Tieleman, D. P.; Sansom, M. S. Simulation studies of the interaction of antimicrobial peptides and lipid bilayers. *Biochim Biophys Acta* **1999**, *1462*, 185-200.
- (15) Biggin, P. C.; Sansom, M. S. Interactions of alpha-helices with lipid bilayers: a review of simulation studies. *Biophys Chem* **1999**, *76*, 161-183.
- (16) Inbaraj, J. J.; Cardon, T. B.; Laryukhin, M.; Grosser, S. M.; Lorigan, G. A. Determining the topology of integral membrane peptides using EPR spectroscopy. *J Am Chem Soc* **2006**, *128*, 9549-9554.
- (17) Harris, E. J.; Pressman, B. C. Obligate cation exchanges in red cells. *Nature* **1967**, *216*, 918-920.
- (18) Sarges, R.; Witkop, B. Gramicidin A. V. The Structure of Valine- and Isoleucine-Gramicidin A. *J Am Chem Soc* **1965**, *87*, 2011-2020.
- (19) Dubos, R. J. Studies on a Bactericidal Agent Extracted from a Soil Bacillus : I. Preparation of the Agent. Its Activity in Vitro. *J Exp Med* **1939**, *70*, 1-10.
- (20) Bradley, R. J.; Urry, D. W.; Okamoto, K.; Rapaka, R. Channel structures of gramicidin: characterization of succinyl derivatives. *Science* **1978**, *200*, 435-437.
- (21) Weinstein, S.; Durkin, J. T.; Veatch, W. R.; Blout, E. R. Conformation of the gramicidin A channel in phospholipid vesicles: a fluorine-19 nuclear magnetic resonance study. *Biochemistry* **1985**, *24*, 4374-4382.
- (22) Wallace, B. A. Structure of gramicidin A. *Biophys J* **1986**, *49*, 295-306.
- (23) Patrick, J. W.; Gamez, R. C.; Russell, D. H. Elucidation of conformer preferences for a hydrophobic antimicrobial peptide by vesicle capture-freeze-drying: a

preparatory method coupled to ion mobility-mass spectrometry. *Anal Chem* **2015**, *87*, 578-583.

(24) Geschwindner, S.; Ulander, J.; Johansson, P. Ligand Binding Thermodynamics in Drug Discovery: Still a Hot Tip? *J Med Chem* **2015**, *58*, 6321-6335.

(25) Abraham, T.; Lewis, R. N.; Hodges, R. S.; McElhaney, R. N. Isothermal titration calorimetry studies of the binding of a rationally designed analogue of the antimicrobial peptide gramicidin S to phospholipid bilayer membranes. *Biochemistry* **2005**, *44*, 2103-2112.

(26) Abraham, T.; Lewis, R. N.; Hodges, R. S.; McElhaney, R. N. Isothermal titration calorimetry studies of the binding of the antimicrobial peptide gramicidin S to phospholipid bilayer membranes. *Biochemistry* **2005**, *44*, 11279-11285.

(27) Schote, U.; Ganz, P.; Fahr, A.; Seelig, J. Interactions of cyclosporines with lipid membranes as studied by solid-state nuclear magnetic resonance spectroscopy and high-sensitivity titration calorimetry. *J Pharm Sci* **2002**, *91*, 856-867.

(28) Maclachlan, I. siRNAs with guts. *Nat Biotechnol* **2008**, *26*, 403-405.

(29) Liang, X.; Mao, G.; Ng, K. Y. Mechanical properties and stability measurement of cholesterol-containing liposome on mica by atomic force microscopy. *J Colloid Interface Sci* **2004**, *278*, 53-62.

(30) Freyer, M. W.; Lewis, E. A. Isothermal titration calorimetry: experimental design, data analysis, and probing macromolecule/ligand binding and kinetic interactions. *Methods Cell Biol* **2008**, *84*, 79-113.

(31) Wiseman, T.; Williston, S.; Brandts, J. F.; Lin, L. N. Rapid measurement of binding constants and heats of binding using a new titration calorimeter. *Anal Biochem* **1989**, *179*, 131-137.

(32) Ruotolo, B. T.; Benesch, J. L.; Sandercock, A. M.; Hyung, S. J.; Robinson, C. V. Ion mobility-mass spectrometry analysis of large protein complexes. *Nat Protoc* **2008**, *3*, 1139-1152.

(33) Fenn, L. S.; Kliman, M.; Mahsut, A.; Zhao, S. R.; McLean, J. A. Characterizing ion mobility-mass spectrometry conformation space for the analysis of complex biological samples. *Anal Bioanal Chem* **2009**, *394*, 235-244.

(34) Valentine, S. J.; Counterman, A. E.; Clemmer, D. E. A database of 660 peptide ion cross sections: use of intrinsic size parameters for bona fide predictions of cross sections. *J Am Soc Mass Spectrom* **1999**, *10*, 1188-1211.

- (35) Seelig, J. Titration calorimetry of lipid-peptide interactions. *Biochim Biophys Acta* **1997**, *1331*, 103-116.
- (36) Wieprecht, T.; Seelig, J. Isothermal titration calorimetry for studying interactions between peptides and lipid membranes. *Curr Top Membr* **2002**, *52*, 31-56.
- (37) Shintou, K.; Nakano, M.; Kamo, T.; Kuroda, Y.; Handa, T. Interaction of an amphipathic peptide with phosphatidylcholine/phosphatidylethanolamine mixed membranes. *Biophys J* **2007**, *93*, 3900-3906.
- (38) Lee, D. K.; Kwon, B. S.; Ramamoorthy, A. Freezing point depression of water in phospholipid membranes: a solid-state NMR study. *Langmuir* **2008**, *24*, 13598-13604.
- (39) Chen, L.; Chen, S. H.; Russell, D. H. An experimental study of the solvent-dependent self-assembly/disassembly and conformer preferences of gramicidin A. *Anal Chem* **2013**, *85*, 7826-7833.
- (40) de Groot, B. L.; Tieleman, D. P.; Pohl, P.; Grubmuller, H. Water permeation through gramicidin A: desformylation and the double helix: a molecular dynamics study. *Biophys J* **2002**, *82*, 2934-2942.
- (41) Woolf, T. B.; Roux, B. Structure, energetics, and dynamics of lipid-protein interactions: A molecular dynamics study of the gramicidin A channel in a DMPC bilayer. *Proteins* **1996**, *24*, 92-114.
- (42) Prenner, E. J.; Lewis, R. N.; Kondejewski, L. H.; Hodges, R. S.; McElhaney, R. N. Differential scanning calorimetric study of the effect of the antimicrobial peptide gramicidin S on the thermotropic phase behavior of phosphatidylcholine, phosphatidylethanolamine and phosphatidylglycerol lipid bilayer membranes. *Biochim Biophys Acta* **1999**, *1417*, 211-223.
- (43) Abraham, T.; Prenner, E. J.; Lewis, R. N.; Mant, C. T.; Keller, S.; Hodges, R. S.; McElhaney, R. N. Structure-activity relationships of the antimicrobial peptide gramicidin S and its analogs: aqueous solubility, self-association, conformation, antimicrobial activity and interaction with model lipid membranes. *Biochim Biophys Acta* **2014**, *1838*, 1420-1429.
- (44) Prenner, E. J.; Lewis, R. N.; Neuman, K. C.; Gruner, S. M.; Kondejewski, L. H.; Hodges, R. S.; McElhaney, R. N. Nonlamellar phases induced by the interaction of gramicidin S with lipid bilayers. A possible relationship to membrane-disrupting activity. *Biochemistry* **1997**, *36*, 7906-7916.